

Novel Azaspirooxindolinone-Based PROTACs for Selective BTK Degradation and Enhanced Anticancer Activity

Naveen Kumar Rampeesa ^[a,b], Rambabu Gundla ^{*[b]}, Gopal Muddasani ^[b], Sudhakar T ^[b], Sreenivasa Reddy Anugu ^[a], Soňa Gurská ^[c, d], Juan Bautista De Sanctis^[c, d], Petr Džubák ^[c, d], Marián Hajdúch ^[c, d], Viswanath Das ^{*[c, d]}

[a] Aragen Life Sciences Ltd, Medicinal Chemistry Laboratory Division, Survey

No: 125(Part) & 126, IDA Mallapur, Hyderabad 500076, India

[b] Department of Chemistry, School of Science, GITAM University, Hyderabad

502102, Telangana, India

[c] Czech Advanced Technologies and Research Institute (CATRIN), Institute of Molecular and Translational Medicine, Palacký University Olomouc, Křížkovského 511/8, 779 00, Olomouc, Czech Republic

[d] Institute of Molecular and Translational Medicine, Faculty of Medicine and Dentistry, Palacký University and University Hospital Olomouc, Hněvotínská 1333/5, 779 00 Olomouc, Czech Republic

*Correspondence to: Viswanath Das (Email: viswanath.das@upol.cz, Tel.: +420 585 632 111; ORCID ID: 0000-0001-5973-5990) and Rambabu Gundla (Email: rgundla@gitam.edu, Tel.: +91-9849869933)

Highlights

- PROTACs degrade ITK and BTK, targeting key disease-related proteins.
- Nine PROTAC derivatives of azaspirooxindolinone were evaluated for cytotoxicity.
- Compounds **7**, **14**, and **25** showed high cytotoxicity (IC₅₀ < 10 μM) against BTK/ITK-positive cell cancer lines.
- PROTAC **25** degraded BTK in RAMOS human B-cell lymphoma cells.
- BTK degradation by PROTAC **25** inhibited downstream signaling.

Keywords

Antiproliferative activity; Azaspirooxindolinone; Bruton's tyrosine kinase; Jurkat; IL-2-inducible T-cell Kinase; PROTAC; Ramos

ABSTRACT

Proteolysis targeting chimera (PROTAC) facilitates the degradation of specific endogenous proteins via the E3 ubiquitin ligase pathway. This study evaluates nine PROTAC derivatives of azaspirooxindolinone targeting IL-2 inducible T cell kinase (ITK) and Bruton's Tyrosine Kinase (BTK), which are implicated in hematological malignancies, autoimmune diseases, allergies, and neuroinflammation. Among all the tested compounds, three (PROTACs **7**, **14**, and **25**) exhibited high cytotoxicity ($IC_{50} < 10 \mu\text{M}$) against BTK- and ITK-positive cancer cell lines, while showing no cytotoxicity against non-cancer fibroblast cells and normal T/B-cell lymphocytes. Despite having the highest docking score of -12.1 kcal/mol , PROTAC **7** did not reduce BTK or ITK protein levels in treated cells. Similarly, PROTAC **14**, with a docking score of -11.2 kcal/mol , and a high cytotoxic against RAMOS cells did not reduce BTK levels. PROTAC **25**, also with a docking score of -11.2 kcal/mol , was notably effective in inducing BTK degradation in a proteasome-dependent manner, which was inhibited in the presence of bortezomib. PROTAC **25** degradation of BTK led to the inhibition of BTK phosphorylation and downstream activation of p38 in lipopolysaccharide and IgM-stimulated RAMOS cells. In conclusion, we report a PROTAC derivative (**25**) of azaspirooxindolinone that shows significant activity against BTK-high cells.

1. INTRODUCTION

The Tec family of non-receptor protein-tyrosine kinases, which includes Bruton's Tyrosine Kinase (BTK) and IL-2 inducible T cell Kinase (ITK), have been extensively studied for decades, particularly for their roles in hematopoietic cells [1]. BTK is one of the widely studied kinases of the Tec family, and its aberrant activity is implicated in various human B-cell malignancies, autoimmune diseases, and neuroinflammation [2–4]. In addition to B cells, this kinase is also expressed in high levels in mast cells, macrophages, and dendritic cells, which are immune cells known to play a role in pathogen clearance [5]. BTK suppression *in vivo* prolongs activated T-cell survival, reducing Treg to $CD4^+$ T-cell ratios, and diminishes immunosuppressive characteristics

of chronic lymphocytic leukemia cells through BTK-dependent and -independent pathways [2]. Studies have also shown the crucial role of BTK in regulating neutrophil functions [6], while clinical trials have demonstrated that inhibiting BTK activity could enhance anti-CD20 treatments, like rituximab, for multiple sclerosis [7,8]. Like BTK, ITK regulates inflammatory responses and has been associated with conditions such as allergic asthma and peripheral T-cell lymphomas [9]. ITK regulates essential signaling pathways involved in inflammatory responses, including the release of cytokines by Th2 cells and mast cells. It plays a regulatory role in calcium-dependent pathways, leading to the activation of transcription factors such as NFAT, NF κ B, and AP1, which control the expression of various inflammatory cytokines, including IL-4, IL-5, IL-13, and IL-2 [10]. Multiple investigations have linked ITK to allergic asthma, dermatitis, peripheral T-cell malignancies, and neuroinflammation [11–13].

Given the involvement of BTK and ITK in various human diseases, focusing on developing innovative inhibitors to modulate their aberrant activity is logical. Proteolysis targeting chimeras (PROTAC) represents an innovative class of heterobifunctional compounds facilitating targeted protein degradation via the E3 ubiquitin ligase pathway [14]. These molecules link the ligands for the protein of interest (POI) and the E3 ubiquitin ligase (E3) through a suitable linker [15]. A recent study successfully developed covalent inhibitor-based PROTACs for the effective degradation of BTK and BLK in live cells, highlighting the importance of optimizing the ligand, linker, and E3 ligase components for efficient protein degradation [16]. Another molecule, MT-802, a CRBN-recruiting PROTAC based on a modified reversible ibrutinib scaffold and pomalidomide moiety, has been developed with higher BTK selectivity than ibrutinib [17].

Furthermore, one of the most widely recognized benefits of the PROTAC modality is its ability to overcome drug resistance caused by mutations. The efficacy of ibrutinib in treating several hematological disorders and chronic graft-versus-host diseases [18,19]. The efficacy of ibrutinib, the first BTK inhibitor for clinical use, relies on its irreversible binding to the C481 site within the ATP-binding pocket, thereby rendering BTK mutations at the C481 site impactful on patient treatment outcomes [19]. An additional advantage of the PROTAC method is its ability to enhance target inhibition through event-driven proteolysis, as opposed to traditional inhibitors [18,20]. Two

orally bioavailable BTK PROTACs have been developed: NX-2127 (NCT04830137), which demonstrates immunomodulatory imide drug activity, and NX-5948 (NCT05131022), which lacks such activity. Both compounds are presently undergoing Phase I clinical trials, with their structures remaining undisclosed. NX-2127 shows promise in treating B-cell malignancies resistant to ibrutinib due to its novel mechanism involving chimeric targeting molecules to degrade BTK, including the C481S mutation [20].

The spirooxindole core has attracted significant interest due to its pharmacological properties, especially in cancer research [21–25]. Building upon our prior work identifying azaspirooxindolinone derivatives with moderate-high activity against BTK-high RAMOS and ITK-positive Jurkat cell lines [26], our study focuses on generating and evaluating nine PROTAC-based derivatives of azaspirooxindolinone by computational and experimental analyses to assess their efficacy in cancer cell lines.

2. Result and discussions

2.1 Chemistry

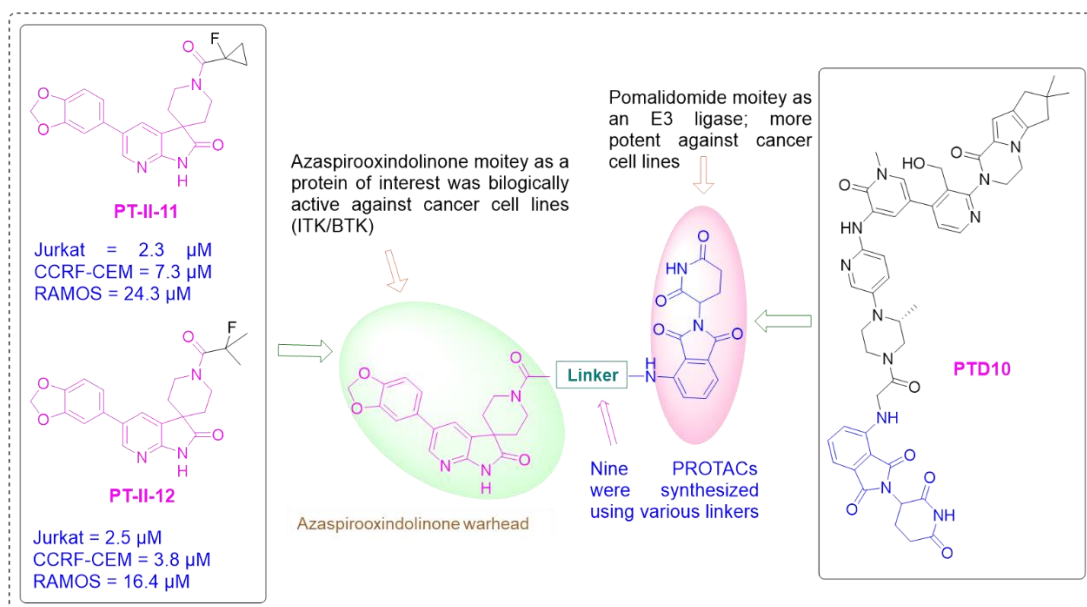
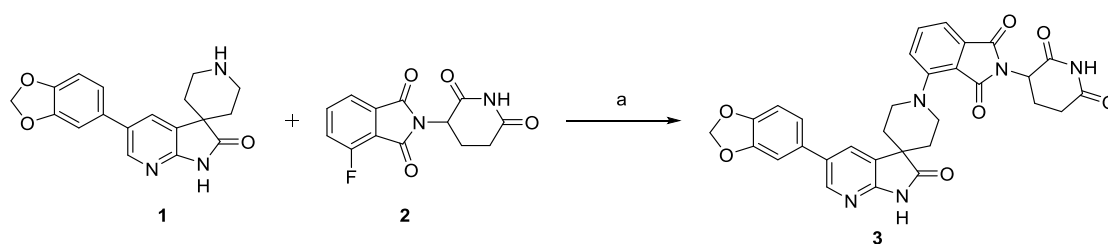


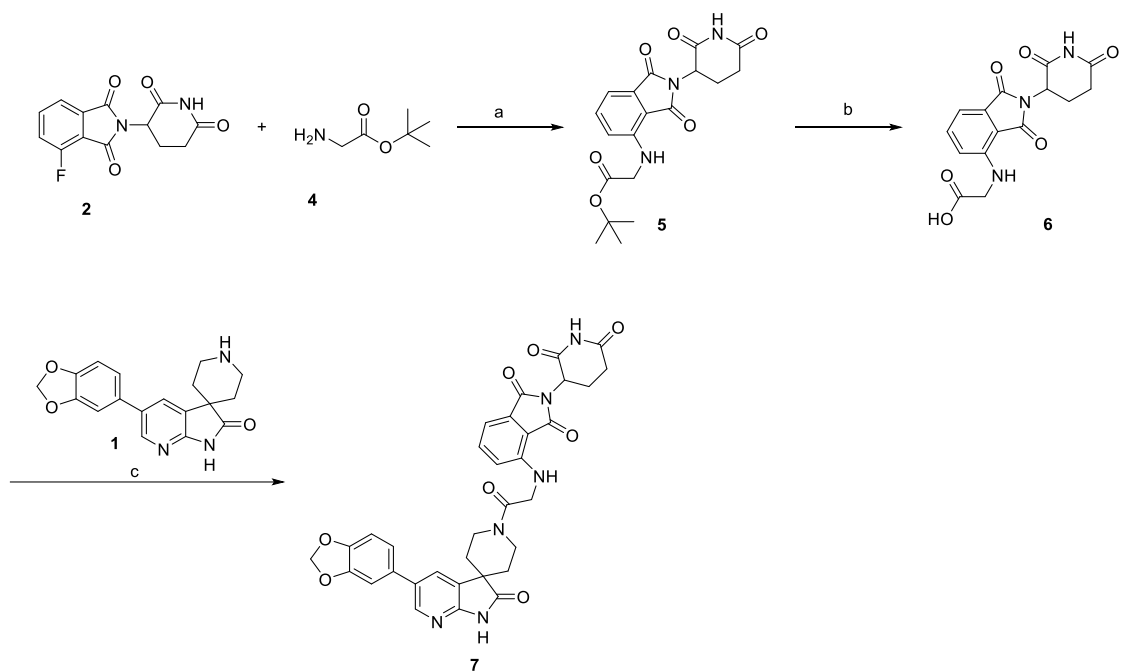
Figure 1. Scheme showing the rational designing of novel azaspirooxindolinone-based PROTACs. Azaspirooxindolinone moiety, from our previous work, was used as a protein of interest Pomalidomide moiety was used as E3 ligase. PTD10 is described in [19] and PT-II-11 and PT-II-12 are described in [21].

The PROTACs were designed based on two azaspirooxindolinone derivatives, PT-II-11 and PT-II-12, previously synthesized by our group, which showed good cytotoxicity against ITK and BTK-positive cancer cell lines [21]. We introduced PROTAC technology to the azaspirooxindolinone moiety to enhance the cytotoxic activity, targeting it as a protein of interest (POI). This moiety was connected via various linkers (PEG, alkyl chain, mixed linker) to a CRBN-based ligand (Pomalidomide) (**Fig. 1**).

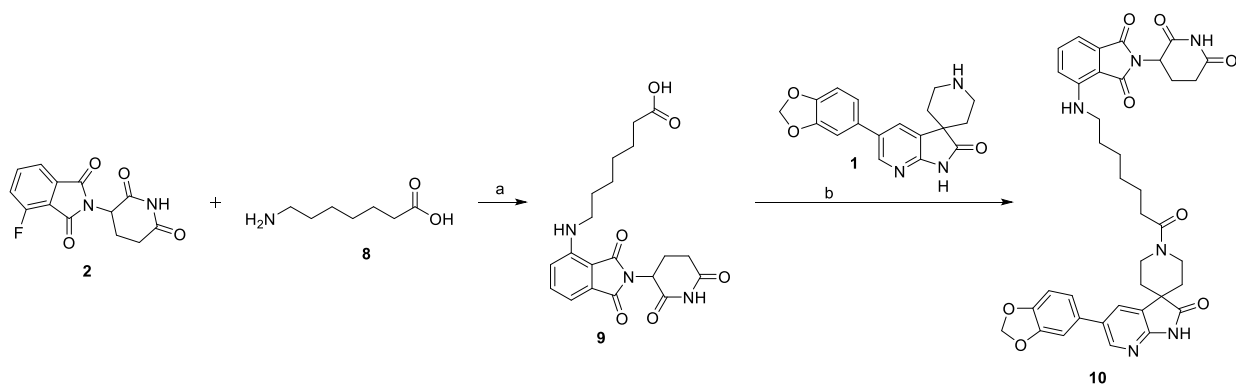
To synthesize compound **3** (**Scheme 1**), azaspirooxindolinone **1** was treated with 5-fluoro thalidomide **2**. For compound **7** (**Scheme 2**), tertiary butyl glycine was first substituted with **2**, followed by tert-butyl deprotection and coupling with **1**. Compound **10** (**Scheme 3**) was prepared by reacting to 7-amino heptanoic acid with **2**, followed by amide coupling with **1**. For compound **14** (**Scheme 4**), nucleophilic substitution of **11** with **2** was followed by deprotection and coupling with **1**. Compound **18** (**Scheme 5**) was synthesized by treating compound **1** with **15**, followed by boc deprotection and substitution with **2**. To obtain compound **21** (**Scheme 6**), 8-amino octanoic acid reacted with **2**, followed by amide coupling with **1**. For compound **25** (**Scheme 7**), compound **1** was reacted with **22**, followed by boc deprotection and substitution with **2**. Similarly, compound **29** (**Scheme 8**) was synthesized by reacting compound **1** with **26**, followed by boc deprotection and substitution with **2**. Finally, for compound **33** (**Scheme 9**), compound **2** was substituted with **30**, followed by tert-butyl deprotection and coupling with **1**. Overall, nine PROTAC compounds were synthesized, out of which a few compounds (**7**, **18**, and **25**) showed good cytotoxic effects (10-20-fold) against BTK/ITK-positive cancer cell lines.



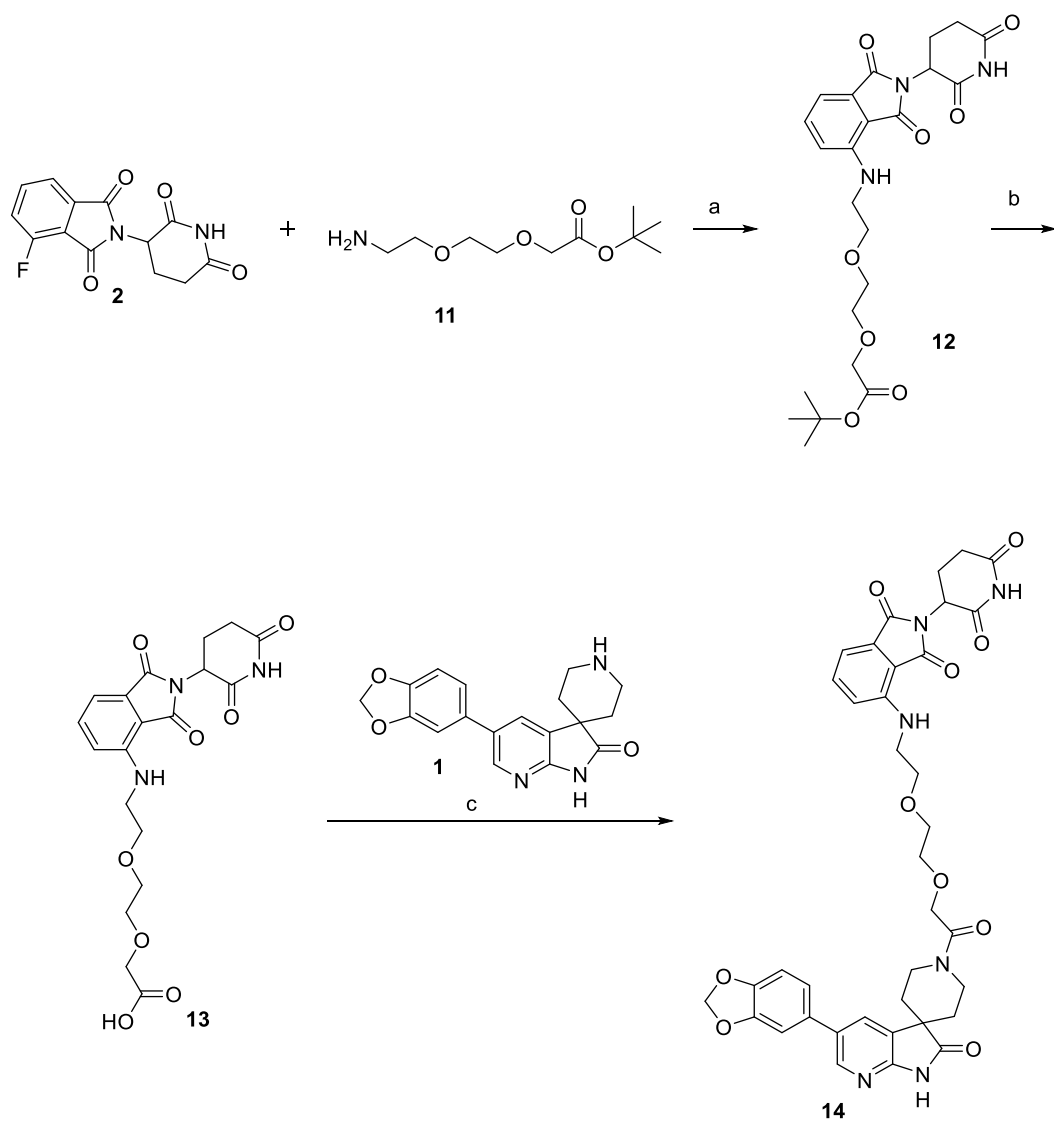
Scheme 1. Synthesis of PROTAC **3**. Reaction condition: a) Diisopropylethylamine (DIPEA), Dimethyl sulfoxide (DMSO), 100 °C.



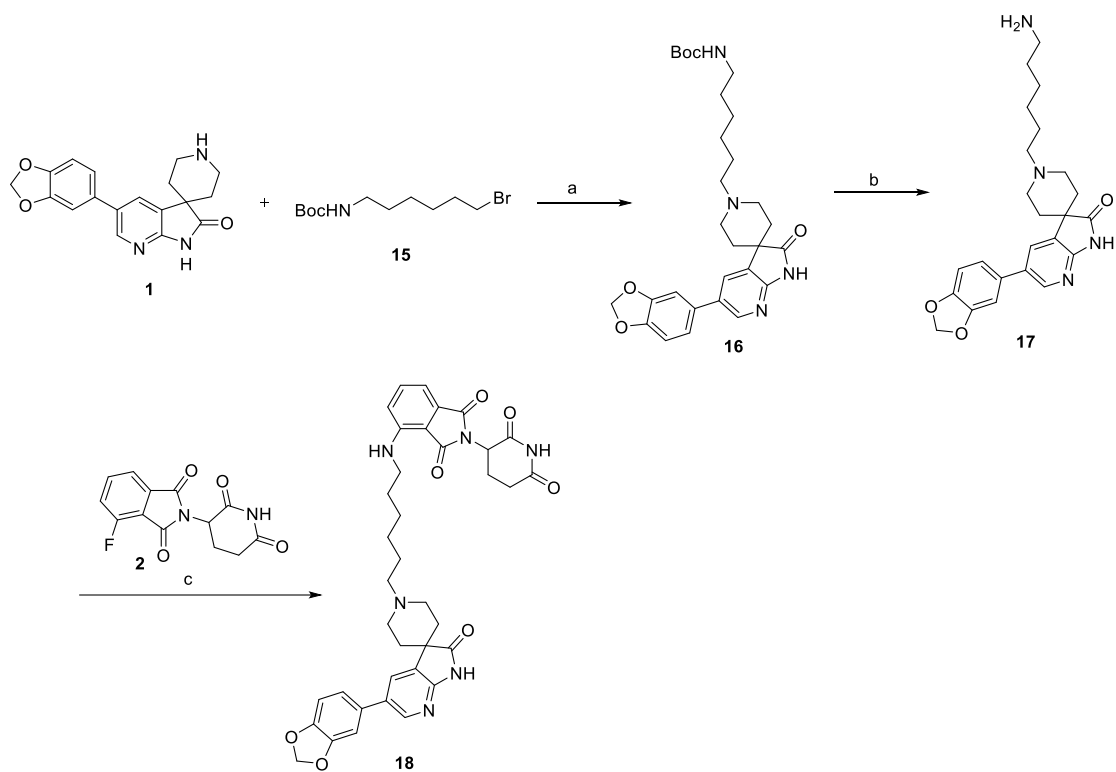
Scheme 2. Synthesis of PROTAC 7. Reaction condition: a) DIPEA, DMSO at 100 °C; b) Trifluoroacetic acid (TFA), Dichloromethane (DCM) at room temperature (RT); c) Hexafluorophosphate azabenzotriazole tetramethyl uronium (HATU), DIPEA, Dimethylformamide (DMF) at RT.



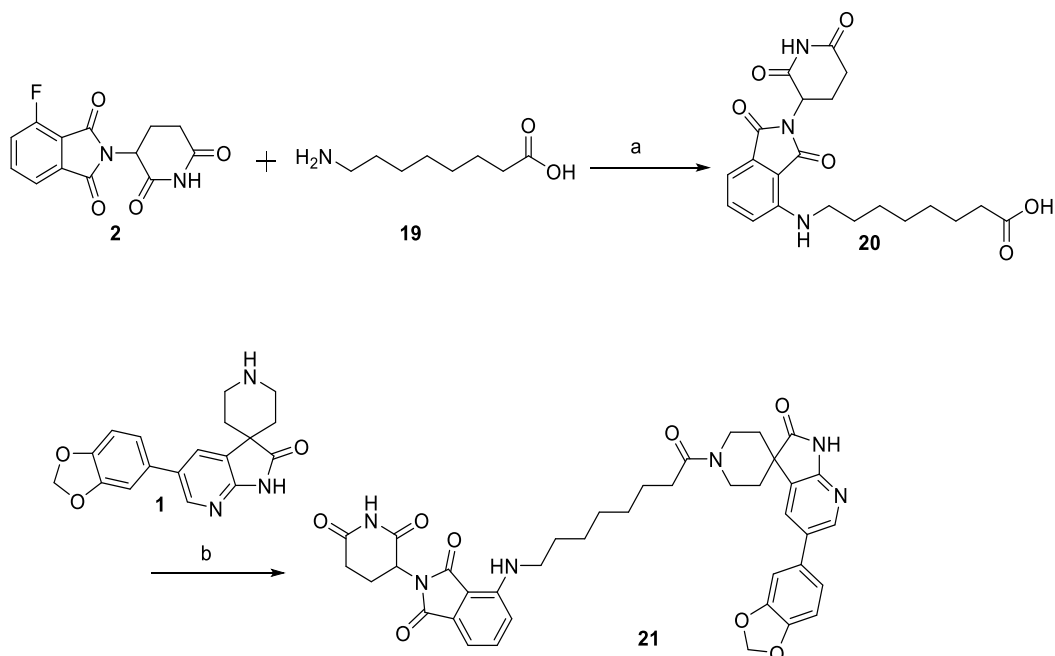
Scheme 3. Synthesis of PROTAC 10. Reaction condition: a) DIPEA, DMSO at 100 °C; b) HATU, DIPEA, DMF at RT.



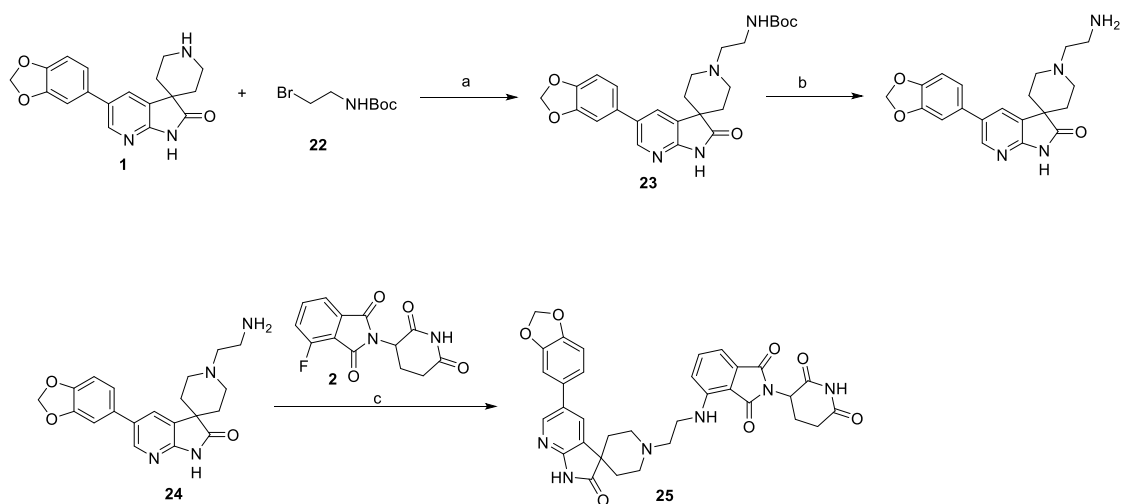
Scheme 4. Synthesis of PROTAC **14**. Reaction condition: a) DIPEA, DMSO at 100 °C; b) TFA, DCM at RT; c) HATU, DIPEA, DMF at RT.



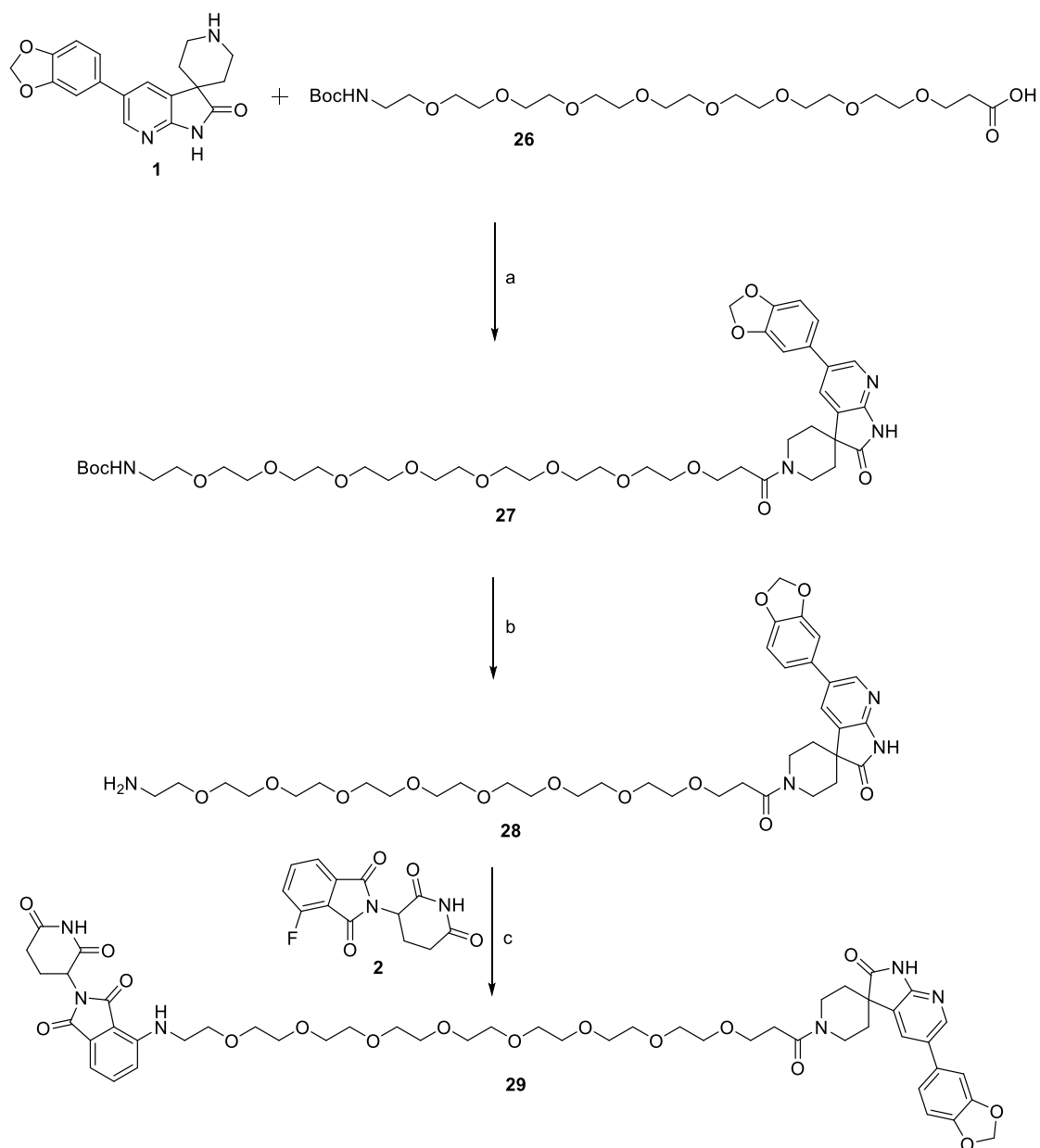
Scheme 5. Synthesis of PROTAC 18. Reaction condition: a) K₂CO₃, DMF at RT; b) TFA, DCM at RT; c) DIPEA, DMSO at RT.



Scheme 6. Synthesis of compound 21. Reaction condition: a) DIPEA, DMSO at 100 °C; b) HATU, DIPEA, DMF at RT.



Scheme 7. Synthesis of PROTAC **25**. Reaction condition: a) K_2CO_3 , DMF at RT; b) TFA, DCM at RT; c) DIPEA, DMSO at 100 °C.



Scheme 8. Synthesis of PROTAC **29**. Reaction condition: a) HATU, DIPEA, DMF at RT; b) TFA, DCM at RT; c) DIPEA, DMSO at 100 °C.

the docking scores and the specific amino acid interactions for each of the tested compounds. PROTAC **3**, **7**, **10**, **14**, **18**, **21**, and **25** showed favorable interactions with key BTK residues, such as Thr474, Leu408, and Arg525, through various types of bonds. These findings are consistent with other studies demonstrating that BTK forms significant hydrogen bonds with residues including Thr474, Met477, Leu408, and Arg525 [27,28]. Notably, PROTAC **25** displayed unique hydrogen bonds with Asp521 and Asn526, which were not observed together in the other PROTACs tested in this study (**Figure 2**). Similar interactions have also been observed with the BTK inhibitor remibrutinib, which forms covalent bonds with residues such as Gln412, Phe413, Asp521, Asn526, and Tyr551 [29]. Due to these interactions with BTK, we next subjected the synthesized compounds to cytotoxicity profiling in a panel of ITK/BTK-null and ITK-BTK-positive cancer cell lines.

Table 1. Docking scores and amino acid interactions of azaspirooxindolinone derivatives with BTK.

PROTAC	Docking Score	Amino Acid Interactions
3	-11.5	Lys558, Tyr551, Asp521, Asn526, Gln412, Gly411, Leu408, Ser538, Val458, Met449, Leu542- van der Waals; Arg525, Thr474- Carbon Hydrogen Bond; Asp539- Pi Anion; Val416, Ala428, Lys430, Ile472, Leu460, Cys481- Pi Alkyl; Leu528- Pi Sigma; Phe540- Pi-Pi T-shaped
7	-12.1	Tyr551, Gly411, Gln412, Asp512, Leu408, Ser538, Leu542, Met449, Asn526, Val458, Leu408- van der Waals; Lys558, Arg525- Conventional Hydrogen Bond; Asp539, Thr474- Carbon Hydrogen Bond; Leu528- Pi Sigma; Phe540- Pi-Pi T-shaped; Val416, Ala428, Lys430, Ile472, Leu460- Pi-Alkyl
10	-10.9	Ile472, Thr474, Glu475, Val458, Tyr476, Met477, Gly480, Gly409, Trp563, Asn603, Thr410, Pro560, Phe559, Cys481, Arg525, Asp521, Gln412, Asn526, Leu542- van der Waals; Lys430, Asp539, Ser538, Lys558- Conventional Hydrogen Bonds; Val416- Pi Sigma; Tyr551- Pi T-shaped; Ala428, Leu528- Pi Alkyl
14	-11.2	Met477, Tyr476, Ser538, Val458, Ile472, Lys430, Asp539, Cys481, Gly409, Thr410, Gly480, Gly411, Asn526, Gln412, Ser543, Pro560, Trp563, Asn603, Asn562- van der Waals; Thr474, Asp521- Conventional Hydrogen Bond; Leu408, Lys558- Carbon Hydrogen Bond; Glu475- Unfavourable Donor; Arg525- Pi Anion; Val416- Pi sigma; Tyr550- Pi-Pi T-shaped; Ala428, Leu528- Pi Alkyl
18	-11.1	Thr474, Val458, Gly411, Ser538, Met477, Tyr476, Gly480, Gly409, Asn526, Leu483- van der Waals; Lys430, Leu408, Arg525- Conventional Hydrogen Bonds; Asn484- Carbon Hydrogen Bonds; Asp539- Pi Anion; Ile472, Ala428, Val416, Leu528, Cys481- Pi Alkyl
21	-11.4	Asn526, Thr474, Val458, Tyr476, Ala478, Gly480, Ser538, Leu408, Thr410, Leu483, Gly411- van der Waals; Met477, Lys430, Cys481, Asn484- Conventional Hydrogen Bond; Glu475, Gly411, Gly409- Carbon Hydrogen Bonds; Asp539- Pi Anion; Ile472, Val416, Leu528, Ala428, Arg525- Pi Alkyl
25	-11.2	Leu408, Tyr551, Gln412, Phe413, Leu542, Gly411, Cys481, Ser538, Phe540, Met449- van der Waals; Asp521, Asn526, Arg525- Conventional Hydrogen Bonds; Lys430- Unfavourable Donor; Thr474- Carbon Hydrogen Bonds; Asp539- Pi Anion; Leu528- Pi Sigma; Ile472, Val458, Leu460, Val416, Ala428- Pi Alkyl

29	-8.4	Met477, Tyr551, Ser538- Conventional Hydrogen Bonds; Lys558, Gly411, Leu435- Carbo Hydrogen Bonds; Asp539, Lys435- Pi Anion; Leu528, Ile432, Val416, Ala428- Pi Alkyl
33	-10.7	Asp521, Phe419, Lys558, Trp563, Met596, Leu483, Thr410, Cys481, Gly409, Ser538, Val458, Glu475, Tyr476, Ala478, Asn484- van der Waals; Arg525, Met477- Conventional Hydrogen Bonds; Asn526, Gly411, Gly480- Carbon Hydrogen Bond; Asp539, Lys430- Pi Anion; Thr474, Leu528- Pi Sulphur; Asp539, Lys430- Pi Anion, Tyr551- Pi-Pi T-Shaped; Leu408, Val416, Ala428, Ile472- Pi Alkyl

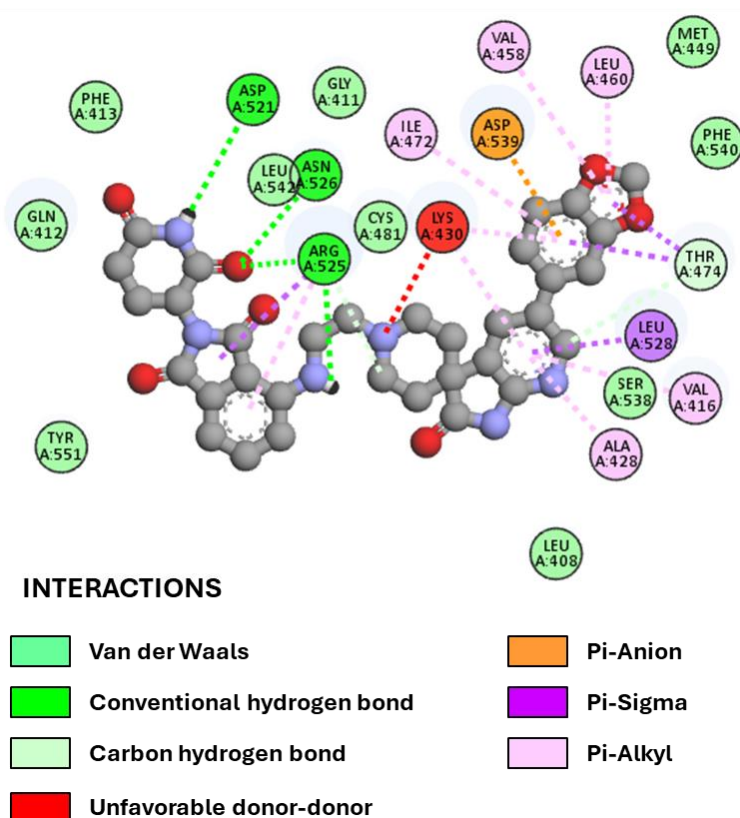


Figure 2. Ligand interaction diagrams for PROTAC 25. The diagram illustrates the binding interactions of PROTAC 25 with the BTK protein, highlighting key residues involved in the interactions. PROTAC 25 forms unique hydrogen bonds with Asp521 and Asn526 (highlighted in the darkest shade of green), which are not observed together in other PROTACs tested in this study.

2.3 Cytotoxicity profiling

The cytotoxic efficacy of all nine azaspirooxindolinone derivatives was evaluated *in vitro* in a panel of cancer and non-cancer cell lines positive or negative for ITK and

BTK expression [30]. Combining glycine as a linker with pomalidomide (**2**) and our POI moiety (**1**), the PROTAC **7** was generated that showed high cytotoxic activity against ITK- and BTK-positive cell lines with IC₅₀ values in the sub-micromolar range (**Table 2**). Further modifications, increasing the linker length to a 6-carbon chain (PROTAC **10**) and a 7-carbon chain (PROTAC **21**), surprisingly led to a loss of anti-cancer activity. Changing the linker to alkyl chains resulted in **18** (6-Methylene) and **25** (2-Methylene) did not alter their cytotoxicity in BTK/ITK-positive cell lines (**Table 2**).

Using an amino-PEG2-acetic acid linker resulted in **14**, resulting in increased cytotoxicity in RAMOS cells ($0.54 \pm 0.14 \mu\text{M}$) than in Jurkat cells ($48 \pm 3.41 \mu\text{M}$). Interestingly, **14** was highly cytotoxic to the other ITK cell line, CCRF-CEM ($0.38 \pm 0.08 \mu\text{M}$). This could be due to the parental CCRF-CEM cell line being highly sensitive to cytotoxic agents [31]. Longer chain PEG8 and PEG6 linkers (PROTACs **29** and **33**) resulted in weak-moderate cytotoxicity against BTK/ITK cell lines. In contrast, **3** without a linker showed no cytotoxic effects in any of the tested BTK/ITK cell lines. Of all derivatives, only **18** showed moderate cytotoxicity against ITK/BTK null cell lines, specifically A549 ($32.70 \pm 6.60 \mu\text{M}$), HCT116 ($22.46 \pm 3.34 \mu\text{M}$), and U2OS ($22.41 \pm 5.32 \mu\text{M}$), possibly suggesting its ITK/BTK non-specificity. None of the active derivatives had any cytotoxicity against non-cancerous MRC-5 and BJ fibroblasts (**Table 2**) or normal T/B-cell lymphocytes (**Table S1**). Overall, incorporating PROTAC technology substantially enhanced the cytotoxic activity of our previously synthesized azaspirooxindolinone derivatives [26].

Table 2. IC₅₀ values of PROTACs in (μM). Data are presented as Mean ± SD, N ≥ 6 for cell lines. Representative IC₅₀ curves of compounds are shown in the supplementary information.

PROTAC	BTK/ITK-null, malignant			ITK-positive, malignant		BTK-positive, malignant		BTK/ITK-null, non-malignant	
	A549	HCT116	U2OS	JURKAT	CCRF-CEM	RAMOS	K562	BJ	MRC-5
3	>50	>50	>50	>50	>50	>50	>50	>50	>50
7	>50	>50	>50	0.73±0.13	0.25±0.03	0.13±0.03	>50	>50	>50
10	>50	>50	>50	>50	>50	>50	>50	>50	>50
14	>50	>50	>50	48.00±3.41	0.38±0.08	0.54±0.14	>50	>50	>50
18	32.70±6.60	22.46±3.34	22.41±5.32	3.52±0.32	2.43±0.28	1.27±0.35	>50	>50	>50
21	>50	>50	>50	>50	>50	>50	>50	>50	>50
25	>50	>50	>50	3.42±0.57	3.81±0.75	9.79±3.39	>50	>50	>50
29	>50	>50	>50	42.00±3.82	35.43±6.89	26.95±3.99	>50	>50	>50
33	>50	>50	>50	39.23±1.31	35.68±3.19	23.54±4.36	>50	>50	>50

2.4 PROTAC effect on Protein Degradation, Phosphorylation, and Downstream Signaling

We selected **7**, **14**, and **25** based on their cytotoxicity profiles for further exploration in RAMOS (B-cell line) and JURKAT (T-cell line) cells (**Figure 3A**). Cells were treated with the compounds at three different concentrations (0.5x, 1x, and 2x IC₅₀) for 72 h, and BTK and ITK levels in whole cell lysates were evaluated by western blotting. Despite having the highest docking score of -12.1 (**Table 1**), **7** did not affect the protein levels of BTK or ITK (**Figure 3B, C**). Similarly, **14** despite showing high cytotoxicity in RAMOS cells, did not reduce BTK protein levels. Of the three PROTACs, **25** specifically decreased BTK levels in RAMOS cells at 1x and 2x IC₅₀ concentrations, with no effect on ITK levels at any tested concentrations in JURKAT cells (**Figure 3B, C**).

To further investigate the BTK-degrading activity of **25**, RAMOS cells were treated with 2x IC₅₀ concentration of the compound in the presence of proteasome inhibitor bortezomib (BTZ) at 10 nM for 24 h. Analysis of whole protein lysate clearly showed that BTZ abolished the BTK-degrading activity of **25** (**Figure 3D**).

Next, to test if BTK degradation blocks downstream signaling, RAMOS cells were first treated with PROTAC **25** for 24 h and then stimulated with lipopolysaccharide (LPS) or IgM for 10 min, followed by analysis of whole protein lysate by western blotting. Previous studies, including ours, have shown that LPS stimulation of RAMOS causes BTK phosphorylation, activating MAPK signaling [30,32]. In cells treated with **25**, there was significantly less phosphorylation of BTK (p-BTK Tyr223) and p38 (p-p38 Thr180/Tyr182) following LPS stimulation (**Figure 3E, F**). Similarly, BTK phosphorylation and activation of BCR signaling cascade in RAMOS cells has also been observed following stimulation with anti-IgM antibody [33,34]. We stimulated RAMOS cells with anti-human IgM antibody for 10 min following 24 h treatment with **25** and observed a decrease in phosphorylation of BTK at Tyr223 and Tyr551 and p38 phosphorylation (p-p38 Thr180/Tyr182) in drug-treated cells (**Figure 3G, H**). Overall, these results show that BTK degradation by PROTAC **25** inhibits the activation downstream BTK-mediated signaling cascade.

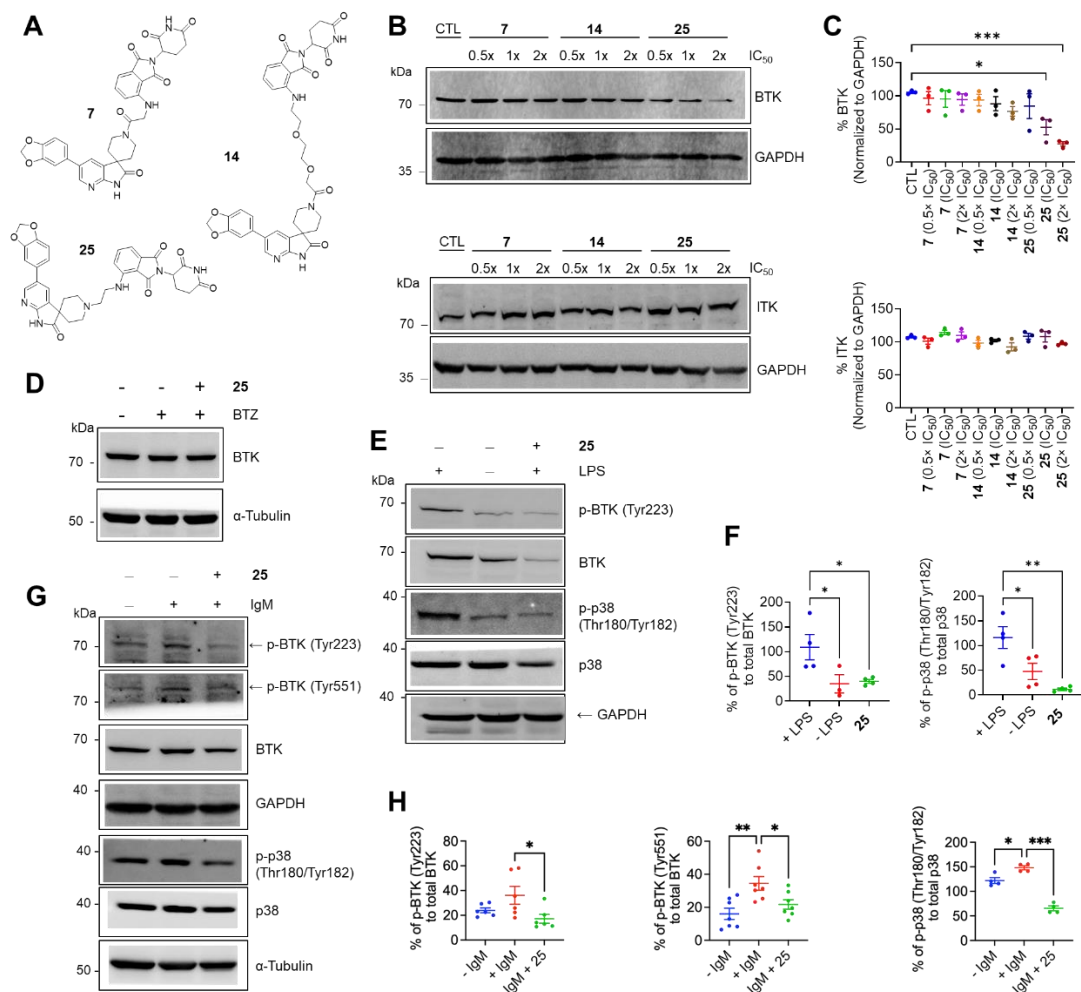


Figure 3. PROTAC 25 degrades BTK levels and inhibits downstream signaling.

(A) Chemical structures of PROTACs **7**, **14**, and **25**. (B) Western blots showing BTK protein levels in RAMOS cells and ITK levels in JURKAT cells following treatment with **7**, **14**, and **25** at the indicated IC_{50} concentrations for 72 h. CTL indicates vehicle (0.05% DMSO)-treated control. (C) Quantification of BTK and ITK levels. Mean \pm SEM (Each dot in the scatter plot represents individual values obtained from 3 independent replicates). (D) Representative immunoblot showing BTZ blocks BTK degradation by **25**. α -Tubulin was used as a loading control. N = 3. (E) PROTAC **25** decreases LPS-mediated phosphorylation of BTK (p-BTK Tyr223) and p38 (p-p38 Thr180/Tyr182). (F) Quantification of p-BTK (Tyr223) to total BTK and p-p38 (Thr180/Tyr182) to total p38. Mean \pm SEM (Each dot in the scatter plot represents individual values obtained from 2 independent replicates). (G) PROTAC **25** prevents IgM-mediated phosphorylation of BTK (p-BTK Tyr223 and Tyr551) and p38 (p-p38 Thr180/Tyr182). (H) Quantification of p-BTK Tyr223 and p-BTK Tyr551 to total BTK and p-p38 Thr180/Tyr182 to total p38. Mean \pm SEM (Each dot in the scatter plot represents individual values obtained from 3 independent replicates). Panels C, F, and H: * $P < 0.05$, ** $P < 0.01$, *** $P < 0.001$, one-way ANOVA, Dunnett's multiple comparisons test. Panel B, D, F, and J: Images of full blots are provided in the supplementary information.

3. Conclusion

We synthesized nine derivatives of azaspirooxindolinone using PROTAC technology to enhance their cytotoxicity against ITK/BTK-positive cancer cell lines. The approach significantly increased the potency of the azaspirooxindolinone derivatives, with PROTACs **7**, **14**, and **25** showing notable activity against ITK/BTK-positive cell lines, but not against ITK/BTK-null cancer cells, fibroblast cells, or primary T- or B-cell lymphocytes. However, both **7** and **14**, despite showing high cytotoxicity in BTK-positive cells, failed to induce BTK degradation. PROTAC **25** emerged as the most effective candidate, inducing BTK degradation in a proteasome-dependent manner, as confirmed by the inhibition of this process in the presence of bortezomib. Additionally, **25** significantly reduced BTK phosphorylation (Tyr233 and Tyr551) and blocked downstream activation of the p38 MAPK pathway, following stimulation with LPS and anti-IgM. Its enhanced activity can be attributed to its effective binding to key BTK residues, Asp521 and Asn526, similar to the BTK inhibitor remibrutinib, which also targets these residues [29]. The specific interaction and subsequent degradation of BTK highlight the potential of **25** as a potent anti-BTK agent for further modification and exploration.

4. Experimental

4.1 Materials and Physical Measurements

All chemicals were purchased from Lancaster (Alfa Aesar, Johnson Matthey Co, Ward Hill, MA, USA), Sigma-Aldrich (St Louis, MO, USA), and Spectrochem Pvt. Ltd (Mumbai, India). Amino acids and amino acid esters were procured from Combi-Blocks, Inc. (San Diego, USA) and BLD Pharm (India). Reactions were monitored by TLC on aluminum plates coated with silica gel and a fluorescent indicator (F254S). Visualization was achieved using UV light, KMnO₄ stain, and iodine indicator.

¹H NMR and ¹³C NMR spectra were recorded on Bruker 400 MHz NMR Magnet (Billerica, Massachusetts, USA). Chemical shifts were reported in ppm, downfield from internal TMS standard. Spectral patterns are designated as follows: s (singlet), d (doublet), dd (doublet of doublets), t (triplet), td (triplet of doublets), bs (broad singlet), m (multiplet).

ESI spectra were recorded on a Microaass Quattro LC using ESI+ software, using a capillary voltage of 3.98 kV and a positive ion trap detector.

IR spectra were recorded on an FT-IR spectrometer, with only major peaks reported in cm^{-1} .

All solutions were prepared in deionized distilled water. All other reagents were of standard quality and commercially available.

4.2 Chemistry

4.2.1 General procedure for amide coupling

To a solution of amine (1.0 equiv.) in DMF (10 v) at 0 °C under a nitrogen atmosphere, acid (1.2 equiv.), HATU (1.5 equiv.), and diisopropylethylamine (DIPEA) (3 equiv.) were added. The resulting reaction mixture was stirred at room temperature for 2 h, and the progress was monitored by TLC. The reaction mixture was then diluted with water (5 mL) and extracted with ethyl acetate (3×10 mL). The combined organic layers were washed with brine (2×10 mL), dried over sodium sulfate, and evaporated to yield the crude product. The crude product was purified using normal phase chromatography with 12 g of silica (REVELERIS) and eluted with 2-5% methanol in DCM. Further purification was carried out using GRACE chromatography with 12 g of C18 (REVELERIS), eluted with a gradient of 30-40% 0.1% FA in water/acetonitrile. The purified fraction was lyophilized to obtain the final product as a solid.

4.2.2 General procedure for substitution reaction

To a solution of 2-(2,6-dioxopiperidin-3-yl)-4-fluoroisindoline-1,3-dione (1 equiv.) in DMSO (10 v), amine (1.2 equiv.) and DIPEA (3 equiv.) in a sealed tube were added at room temperature. The reaction mixture was stirred at 100 °C for 1 h and monitored by TLC. After completion, the reaction mixture was poured into water (5 mL) and extracted with ethyl acetate (3×10 mL). The combined organic layers were washed with brine (2×10 mL), dried over sodium sulfate, and evaporated to yield the crude product. The crude product was purified by GRACE chromatography using 12 g of silica (REVELERIS) with a gradient of 50-100% ethyl acetate in pet ether to afford the final product.

4.2.3 General procedure for global de-protection of Boc and tertiary butyl ester groups

To a solution of Boc-protected amine or tertiary butyl ester in dry DCM (10 v) at 0 °C, TFA (5 equiv.) was added. The reaction mixture was stirred at room temperature for 16 h and monitored by TLC. After the reaction was complete, the mixture was concentrated under reduced pressure to remove volatiles. It was then co-distilled with diethyl ether to obtain the TFA salt of the product. This TFA salt was used directly in the next step without further purification.

4.2.4 General procedure for N-alkylation reaction

To a solution of amine (1 equiv.) in DMF (10 v) the bromo derivative (1.2 equiv.) and potassium carbonate (1.5 equiv.) were added. The reaction mixture was stirred at room temperature for 16 h and monitored by TLC. After the reaction was complete, the mixture was poured into water (5 mL) and extracted with ethyl acetate (3 × 10 mL). The combined organic layers were washed with brine (2 × 5 mL), dried over sodium sulfate, and evaporated to yield the crude product. The crude product was purified by Biotage chromatography using 12 g of silica (REVELERIS) with a gradient of 2-5% methanol in DCM to obtain the final product.

4.2.4.1. Procedure for 5'-(benzo[d][1,3]dioxol-5-yl)spiro[piperidine-4,3'-pyrrolo[2,3-b]pyridin]-2'(1'H)-one (Compound 1)

This compound **1** was prepared using the procedure reported previously [35].

4.2.4.2. Procedure for 2-(2,6-dioxopiperidin-3-yl)-4-fluoroisoindoline-1,3-dione (Compound 2)

A mixture of 4-fluoroisobenzofuran-1,3-dione (2 g, 12.19 mmol), 3-aminopiperidine-2,6-dione hydrochloride (2.02 g, 12.19 mmol), and sodium acetate (1.5 g, 18.29 mmol) in acetic acid (20 mL) was stirred at 135 °C for 16 h. The reaction mixture was then cooled and concentrated under reduced pressure. The residue was suspended in water (100 mL) and stirred at room temperature for 2 h. The resulting solid was collected by filtration and dried under vacuum to yield 2-(2,6-dioxopiperidin-3-yl)-4-

fluoroisindoline-1,3-dione (**2**) as a beige solid (3.0 g, 91% yield). *MS*: m/z ($M+H$)⁺: 277.25. This compound **2** was prepared using the reported procedure [36].

4.2.4.3. Procedure for (4-(5'-(benzo[d][1,3]dioxol-5-yl)-2'-oxo-1',2'-dihydrospiro[piperidine-4,3'-pyrrolo[2,3-b]pyridin]-1-yl)-2-(2,6-dioxopiperidin-3-yl)isindoline-1,3-dione (Compound 3)

To a solution of 2-(2,6-dioxopiperidin-3-yl)-4-fluoroisindoline-1,3-dione (**2**) (42.7 mg, 0.154 mmol, 1.0 equiv.) and 5'-(benzo[d][1,3]dioxol-5-yl)spiro[piperidine-4,3'-pyrrolo[2,3-b]pyridin]-2'(1H)-one (**1**) (50 mg, 0.154 mmol, 1.0 equiv.) in DMSO (0.5 mL), DIPEA (0.08 mL, 0.467 mmol, 3 equiv.) was added. The reaction mixture was stirred at 100 °C for 1 h and monitored by TLC and LC-MS. Upon completion, the reaction mixture was cooled, diluted with ethyl acetate (10 mL), and washed with water (3 × 5 mL). The organic layer was separated, washed with brine, dried over sodium sulfate, filtered, and concentrated under reduced pressure to yield the crude product. The crude product was purified twice by GRACE reverse-phase chromatography using 12 g of C18 silica (REVELERIS), eluted with a gradient of 20-30% acetonitrile in 0.1% formic acid in water. The collected fractions were lyophilized to afford 4-(5'-(benzo[d][1,3]dioxol-5-yl)-2'-oxo-1',2'-dihydrospiro[piperidine-4,3'-pyrrolo[2,3-b]pyridin]-1-yl)-2-(2,6-dioxopiperidin-3-yl)isindoline-1,3-dione (**3**) (10 mg, 10%) as a pale yellow solid. *¹H-NMR (400 MHz, DMSO-*d*₆)*: δ 11.15 (s, 1H), 11.08 (s, 1H), 8.34 (m, 1H), 8.14 (s, 1H), 7.73 (t, *J* = 7.6 Hz, 1H), 7.47 (d, *J* = 8.4 Hz, 1H), 7.38-7.33 (m, 2H), 7.18 (d, *J* = 8.0 Hz, 1H), 6.99 (d, *J* = 8.0 Hz, 1H), 6.05 (s, 2H), 5.13-5.08 (m, 1H), 3.74-3.62 (m, 4H), 2.89-2.87 (m, 1H), 2.67-2.55 (m, 2H), 2.05-2.02 (m, 5H); *¹³C-NMR (400 MHz, DMSO-*d*₆)*: 180.5, 172.7, 170.0, 167.3, 166.3, 155.0, 150.0, 147.9, 146.7, 144.1, 135.7, 133.6, 131.6, 129.9, 129.6, 128.5, 124.2, 120.1, 116.3, 114.6, 108.6, 107.1, 101.0, 69.7, 48.7, 46.2, 46.1, 45.0. 31.9, 30.9, 22.0. *LC-MS (ES-API)*: m/z = 580.1 ($M+H$)⁺.

4.2.4.4 Preparation of tert-butyl (2-(2,6-dioxopiperidin-3-yl)-1,3-dioxoisindolin-4-yl)glycinate (Compound 5)

To a solution of 2-(2,6-dioxopiperidin-3-yl)-4-fluoroisindoline-1,3-dione (**2**) (50 mg, 0.181 mmol, 1.0 equiv.) and tert-butyl glycine (**4**) (28 mg, 0.217 mmol, 1.2 equiv.) in DMSO (0.5 mL), DIPEA (0.1 mL, 0.543 mmol, 3.0 equiv.) was added at room

temperature. The reaction mixture was stirred at 100 °C for 1 h and monitored by TLC and LC-MS. Upon completion of the reaction, the mixture was cooled, diluted with water (10 mL), and extracted with ethyl acetate (3 × 15 mL). The organic layer was separated, washed with water and brine, dried over sodium sulfate, filtered, and concentrated under reduced pressure to yield the crude product. The crude product was purified by GRACE chromatography using 12 g of silica (REVELERIS), eluted with a gradient of 40-50% ethyl acetate in pet ether. The purified product (64 mg, 64% yield) was obtained as a pale yellow foamy solid and identified as tert-butyl (2-(2,6-dioxopiperidin-3-yl)-1,3-dioxoisindolin-4-yl)glycinate (**5**). *¹H-NMR (400 MHz, CDCl₃):* δ 7.95 (bs, 1H), 7.51 (t, *J* = 8.0 Hz, 1H), 7.16 (d, *J* = 7.2 Hz, 1H), 6.77-6.71 (m, 2H), 4.94-4.90 (m, 1H), 3.98 (d, *J* = 6.0 Hz, 2H), 2.98-2.61 (m, 3H), 2.14-2.11 (m, 1H), 1.50 (m, 9H); *LC-MS (ES-API):* *m/z* = 388.2 (M+H)⁺.

4.2.4.5. Preparation of (2-(2,6-dioxopiperidin-3-yl)-1,3-dioxoisindolin-4-yl)glycine (Compound 6)

To a solution of tert-butyl (2-(2,6-dioxopiperidin-3-yl)-1,3-dioxoisindolin-4-yl)glycinate (**5**) (100 mg, 0.258 mmol, 1.0 equiv.) in DCM (1 mL) at 0 °C, TFA (0.147 mL, 1.291 mmol, 5.0 equiv.) was added. The reaction mixture was stirred at room temperature for 16 h and monitored by TLC and LC-MS. After completion, the reaction mixture was concentrated under reduced pressure and co-distilled with diethyl ether to obtain the crude product, (2-(2,6-dioxopiperidin-3-yl)-1,3-dioxoisindolin-4-yl)glycine (**6**) (100 mg) as a pale-yellow viscous liquid. This crude product was used directly in the next step without further purification. *LC-MS (ES-API):* *m/z* = 332.5 (M+H)⁺, as reported previously [37].

4.2.4.6. Preparation of 4-((2-(5'-(benzo[d][1,3]dioxol-5-yl)-2'-oxo-1',2'-dihydrospiro[piperidine-4,3'-pyrrolo[2,3-b]pyridin]-1-yl)-2-oxoethyl)amino)-2-(2,6-dioxopiperidin-3-yl)isindoline-1,3-dione (Compound 7)

To a stirred solution of 5'-(benzo[d][1,3]dioxol-5-yl)spiro[piperidine-4,3'-pyrrolo[2,3-b]pyridin]-2'(1'H)-one (**1**) (100 mg, 0.309 mmol, 1.0 equiv.) in DMF (1 mL) at 0 °C under a nitrogen atmosphere, (2-(2,6-dioxopiperidin-3-yl)-1,3-dioxoisindolin-4-yl)glycine (**6**) (100 mg, 0.309 mmol, 1.0 equiv.), HATU (172 mg, 0.465 mmol, 1.5 equiv.), and DIPEA (0.26 mL, 1.54 mmol, 5.0 equiv.) were added. The reaction mixture

was stirred at RT for 2 h and monitored by TLC. After completion, the mixture was diluted with water (5 mL) and extracted with ethyl acetate (3 × 15 mL). The combined organic layers were washed with brine (2 × 10 mL), dried over sodium sulfate, and evaporated to yield the crude product. The crude product was purified twice by GRACE reverse-phase chromatography using 12 g of C18 silica (REVELERIS) and eluted with a gradient of 35-40% acetonitrile in 0.1% formic acid in water. The collected fractions were lyophilized to obtain 4-((2-(5'-(benzo[d][1,3]dioxol-5-yl)-2'-oxo-1',2'-dihydrospiro[piperidine-4,3'-pyrrolo[2,3-b]pyridin]-1-yl)-2-oxoethyl)amino)-2-(2,6-dioxopiperidin-3-yl)isoindoline-1,3-dione (**7**) as a pale-yellow solid (40 mg, 21% yield). ¹H-NMR (500 MHz, DMSO-d₆): δ 11.17 (bs, 1H), 11.08 (s, 1H), 8.34 (s, 1H), 8.10 (s, 1H), 7.62 (t, *J* = 8.0 Hz, 1H), 7.31 (s, 1H), 7.18-7.16 (m, 3H), 7.08 (d, *J* = 7.0 Hz, 1H), 6.98 (d, *J* = 8.0 Hz, 1H), 6.04 (s, 2H), 5.09-5.05 (m, 1H), 4.34-4.31 (m, 1H), 4.30-4.19 (m, 1H), 3.99-3.16 (m, 1H), 3.89-3.83 (m, 3H), 2.89-2.86 (m, 1H), 2.69-2.55 (m, 1H), 2.05-2.03 (m, 1H), 1.95-1.75 (m, 1H); ¹³C-NMR (500 MHz, DMSO-d₆): 180.5, 172.8, 170.1, 168.8, 167.3, 166.4, 155.2, 147.9, 146.7, 145.3, 144.1, 136.1, 132.0, 131.6, 129.8, 129.5, 128.2, 119.9, 118.2, 110.7, 109.5, 108.6, 106.9, 101.1, 48.5, 45.1, 43.7, 37.3, 31.6, 31.2, 30.9, 22.15; LC-MS (ES-API): *m/z* = 637.2 (M+H)⁺. IR: 1708.9 cm⁻¹ (C=O stretching); MR: 215-218 °C.

4.2.4.7. Preparation of 7-((2-(2,6-dioxopiperidin-3-yl)-1,3-dioxoisindolin-4-yl)amino)heptanoic acid (Compound 9)

To a solution of 2-(2,6-dioxopiperidin-3-yl)-4-fluoroisoindoline-1,3-dione **2** (100 mg, 0.362 mmol, 1.0 equiv.) and 7-aminoheptanoic acid **8** (63 mg, 0.434 mmol, 1.2 equiv., BLD pharma) in DMSO (1 mL), DIPEA (0.31 mL, 1.81 mmol, 5 equiv.) was added at room temperature. The resulting reaction mixture was stirred at 100 °C for 1 h and monitored by TLC and LC-MS. After completion of the reaction, the reaction mixture was cooled, diluted with water (5 mL), and extracted with ethyl acetate (3 × 10 mL). The separated organic layer was washed with water, then with brine, and dried over sodium sulfate. It was then filtered and concentrated under reduced pressure to afford crude product. This crude product was purified by GRACE chromatography (12 g, Silica (REVELERIS)) and eluted with 5-10% of methanol in DCM. The final product was 7-((2-(2,6-dioxopiperidin-3-yl)-1,3-dioxoisindolin-4-yl)amino)heptanoic acid **9**,

in the form of a pale yellow foamy solid to get (52 mg, 35%) [38]. *LC-MS (ES-API)*: $m/z = 402.2$ (M+H)⁺.

4.2.4.8. Preparation of 4-((7-(5'-(benzo[d][1,3]dioxol-5-yl)-2'-oxo-1',2'-dihydrospiro[piperidine-4,3'-pyrrolo[2,3-b]pyridin]-1-yl)-7-oxoheptyl)amino)-2-(2,6-dioxopiperidin-3-yl)isoindoline-1,3-dione (Compound 10)

To a stirred solution of 5'-(benzo[d][1,3]dioxol-5-yl)spiro[piperidine-4,3'-pyrrolo[2,3-b]pyridin]-2'(1H)-one **1** (40 mg, 0.123 mmol) in DMF (0.5 mL) at 0 °C under nitrogen atmosphere, 7-((2-(2,6-dioxopiperidin-3-yl)-1,3-dioxoisindolin-4-yl)amino)heptanoic acid **9** (40 mg, 0.123 mmol), HATU (70 mg, 1.84 mmol, 1.5 equiv.) and DIPEA (0.064 mL, 0.369 mmol, 3 equiv.) were added. The reaction mixture was stirred at room temperature for 2 h, and the progress was monitored by TLC. The reaction mixture was then diluted with water (5 mL) and extracted with ethyl acetate (3 x 10 mL). The combined organic layer was washed with brine (2 x 10 mL), dried over sodium sulfate, and evaporated to yield the crude product. This crude product was purified by GRACE chromatography using 12 g of C18 (REVELERIS) using 35-40% of acetonitrile/0.1% FA in water. The collected fraction was lyophilized to obtain 4-((7-(5'-(benzo[d][1,3]dioxol-5-yl)-2'-oxo-1',2'-dihydrospiro[piperidine-4,3'-pyrrolo[2,3-b]pyridin]-1-yl)-7-oxoheptyl)amino)-2-(2,6-dioxopiperidin-3-yl)isoindoline-1,3-dione **10** as a pale-yellow solid (25 mg, 29%). *¹H-NMR (400 MHz, DMSO-*d*₆)*: δ 11.17 (s, 2H), 8.53 (s, 1H), 8.33 (m, 1H), 8.10 (s, 1H), 7.57 (t, $J = 8.4$ Hz, 1H), 7.32 (s, 1H), 7.17 (dd, $J = 1.6$ Hz, 8.4 Hz, 1H), 7.10 (d, $J = 8.4$ Hz, 1H), 7.02-6.67 (m, 2H), 6.54 (t, $J = 6.4$ Hz, 1H), 6.05 (s, 2H), 5.06-5.02 (m, 1H), 3.83-3.75 (m, 4H), 3.31-3.30 (m, 2H, merged with moisture), 2.87-2.84 (m, 1H), 2.59-2.55 (m, 2H), 2.39-2.33 (m, 2H), 2.03-2.00 (m, 1H), 1.81-1.73 (m, 4H), 1.61-1.50 (m, 4H), 1.49-1.32 (m, 4H). *LC-MS (ES-API)*: $m/z = 707.2$ (M+H)⁺. *IR*: 1701.2 cm⁻¹ (C=O stretching). *MR*: 197-200 °C.

4.2.4.9. Preparation of tert-butyl 2-(2-(2-((2-(2,6-dioxopiperidin-3-yl)-1,3-dioxoisindolin-4-yl)amino)ethoxy)ethoxy)acetate (Compound 12)

To a solution of 2-(2,6-dioxopiperidin-3-yl)-4-fluoroisoindoline-1,3-dione (**2**) (130 mg, 0.471 mmol) and compound **11** (123 mg, 0.565 mmol, 1.2 equiv., BLD Pharma) in DMSO (1.3 mL), DIPEA (0.25 mL, 1.41 mmol, 3.0 equiv.) was added at room

temperature. The reaction mixture was stirred at 100 °C for 1 h and monitored by TLC and LC-MS. Upon completion, the reaction mixture was cooled, diluted with water (5 mL), and extracted with ethyl acetate (2 × 10 mL). The separated organic layer was washed with water and brine, dried over sodium sulfate, filtered, and concentrated under reduced pressure to yield the crude product. The crude product was purified by GRACE chromatography using 12 g of silica (REVELERIS), eluted with a gradient of 5-10% methanol in DCM. The purified product (65 mg, 29% yield) was tert-butyl 2-(2-(2-((2-(2,6-dioxopiperidin-3-yl)-1,3-dioxoisindolin-4-yl)amino)ethoxy)ethoxy)acetate (**12**) as a pale-yellow solid. ¹H-NMR (400 MHz, CDCl₃): δ 7.92 (s, 1H), 7.50 (t, *J* = 8.0 Hz, 1H), 7.10 (d, *J* = 7.2 Hz, 1H), 6.93 (d, *J* = 8.4 Hz, 1H), 6.49-6.47 (m, 1H), 4.93-4.88 (m, 1H), 4.11 (s, 2H), 3.75-3.71 (m, 6H), 3.61-3.46 (m, 2H), 2.91-2.72 (m, 3H), 2.14-2.11 (m, 1H), 1.47 (m, 9H); LC-MS (ES-API): *m/z* = 476.2 (M+H)⁺.

4.2.4.10. Preparation of 2-(2-(2-((2-(2,6-dioxopiperidin-3-yl)-1,3-dioxoisindolin-4-yl)amino)ethoxy)ethoxy)acetic acid (Compound 13)

To a solution of tert-butyl 2-(2-(2-((2-(2,6-dioxopiperidin-3-yl)-1,3-dioxoisindolin-4-yl)amino)ethoxy)ethoxy)acetate (**12**) (65 mg, 0.136 mmol) in DCM (1 mL), TFA (0.078 mL, 0.684 mmol, 5.0 equiv.) was added at 0 °C. The reaction mixture was stirred at room temperature for 16 h and monitored by TLC and LC-MS. Upon completion, the reaction mixture was concentrated under reduced pressure and co-distilled with diethyl ether to yield the crude product (80 mg) as 2-(2-(2-((2-(2,6-dioxopiperidin-3-yl)-1,3-dioxoisindolin-4-yl)amino)ethoxy)ethoxy)acetic acid (**13**) as a pale-yellow viscous liquid. This crude product was used directly in the next step without further purification. LC-MS (ES-API): *m/z* = 420.2 (M+H)⁺, as reported previously [38].

4.2.4.11. Preparation of 4-((2-(2-(2-(5'-(benzo[d][1,3]dioxol-5-yl)-2'-oxo-1',2'-dihydrospiro[piperidine-4,3'-pyrrolo[2,3-b]pyridin]-1-yl)-2-oxoethoxy)ethoxy)ethyl)amino)-2-(2,6-dioxopiperidin-3-yl)isoindoline-1,3-dione (Compound 14)

To a stirred solution of 5'-(benzo[d][1,3]dioxol-5-yl)spiro[piperidine-4,3'-pyrrolo[2,3-b]pyridin]-2'(1H)-one (**1**) (75 mg, 0.185 mmol) in DMF (0.5 mL) at 0 °C under a nitrogen atmosphere, 2-(2-(2-((2-(2,6-dioxopiperidin-3-yl)-1,3-dioxoisindolin-4-

yl)amino)ethoxy)ethoxy)acetic acid (**13**) (60 mg, 0.185 mmol), HATU (105 mg, 0.277 mmol, 1.5 equiv.), and DIPEA (0.09 mL, 0.55 mmol, 3.0 equiv.) were added. The reaction mixture was stirred at room temperature for 2 h and monitored by TLC. After the reaction was complete, the mixture was diluted with water (5 mL) and extracted with ethyl acetate (3 × 12 mL). The combined organic layers were washed with brine (2 × 10 mL), dried over sodium sulfate, and evaporated to yield the crude product. The crude product was purified twice by GRACE reverse-phase chromatography using 12 g of C18 silica (REVELERIS) and eluted with a gradient of 35-40% acetonitrile in 0.1% formic acid in water. The collected fractions were lyophilized to obtain 4-((2-(2-(2-(5'-(benzo[d][1,3]dioxol-5-yl)-2'-oxo-1',2'-dihydrospiro[piperidine-4,3'-pyrrolo[2,3-b]pyridin]-1-yl)-2-oxoethoxy)ethoxy)ethyl)amino)-2-(2,6-dioxopiperidin-3-yl)isoindoline-1,3-dione (**14**) as a pale-yellow solid (20 mg, 15% yield). **¹H-NMR (400 MHz, DMSO-*d*₆)**: δ 11.17 (bs, 1H), 11.08 (s, 1H), 8.35 (s, 1H), 8.10 (s, 1H), 7.56 (t, *J* = 8.4 Hz, 1H), 7.31 (s, 1H), 7.17-7.11 (m, 2H), 7.00 (dd, *J* = 17.6, 8.4 Hz, 2H), 6.54 (t, *J* = 6.4 Hz, 1H), 6.04 (s, 2H), 5.05-5.00 (m, 1H), 4.26-4.17 (m, 2H), 3.85-3.76 (m, 3H), 3.65-3.62 (m, 7H), 3.47-3.46 (m, 2H), 2.85-2.81 (m, 1H), 2.02-1.98 (m, 2H), 1.82-1.75 (m, 4H); **¹³C-NMR (400 MHz, DMSO-*d*₆)**: 180.3, 172.7, 170.0, 168.9, 167.3, 167.2, 154.9, 147.9, 146.7, 146.3, 144.1, 136.1, 132.0, 131.5, 129.9, 129.5, 128.2, 120.0, 117.3, 110.6, 109.2, 108.6, 107.0, 101.1, 69.8, 69.5, 68.8, 48.5, 45.3, 41.7, 36.7, 31.9, 31.2, 30.9, 22.1. IR: 1701.2 cm⁻¹(C=O stretching); **LC-MS (ES-API)**: *m/z* = 725.3 (M+H)⁺. **IR**: 1701.2 cm⁻¹(C=O stretching). **MR**: 167-169 °C.

4.2.4.12. Preparation of tert-butyl (6-(5'-(benzo[d][1,3]dioxol-5-yl)-2'-oxo-1',2'-dihydrospiro[piperidine-4,3'-pyrrolo[2,3-b]pyridin]-1-yl)hexyl)carbamate (Compound 16)

To a solution of 5'-(benzo[d][1,3]dioxol-5-yl)spiro[piperidine-4,3'-pyrrolo[2,3-b]pyridin]-2'(1'H)-one (**1**) (50 mg, 0.154 mmol) and tert-butyl (6-bromohexyl)carbamate (**15**) (43 mg, 0.154 mmol, 1.0 equiv., BLD Pharma) in DMF (1 mL) at 0 °C, potassium carbonate (42 mg, 0.308 mmol) was added. The reaction mixture was stirred at room temperature for 16 h and monitored by TLC and LC-MS. Upon completion, the reaction mixture was diluted with water (10 mL) and extracted with ethyl acetate (2 × 15 mL). The separated organic layer was washed with water and brine, dried over sodium sulfate, filtered, and concentrated under reduced pressure to

obtain the crude product. The crude product was purified by GRACE chromatography using 12 g of silica (REVELERIS) and eluted with a gradient of 2-5% methanol in DCM to yield tert-butyl (6-(5'-(benzo[d][1,3]dioxol-5-yl)-2'-oxo-1',2'-dihydrospiro[piperidine-4,3'-pyrrolo[2,3-b]pyridin]-1-yl)hexyl)carbamate (**16**) as a pale-yellow solid (75 mg, 93% yield). ¹H-NMR (400 MHz, CDCl₃): δ 8.44 (bs, 1H), 8.27 (d, *J* = 2.0 Hz, 1H), 7.76 (d, *J* = 2.0 Hz, 1H), 6.97-6.95 (m, 2H), 6.90 (d, *J* = 8.0 Hz, 1H), 6.02 (s, 2H), 4.52 (m, 1H), 3.11-2.54 (m, 8H), 2.06-1.89 (m, 4H), 1.53-1.36 (m, 18H); LC-MS (ES-API): *m/z* = 523.3 (M+H)⁺.

4.2.4.13. Preparation of 1-(6-aminohexyl)-5'-(benzo[d][1,3]dioxol-5-yl)spiro[piperidine-4,3'-pyrrolo[2,3-b]pyridin]-2'(1'H)-one (Compound 17)

To a solution of tert-butyl (6-(5'-(benzo[d][1,3]dioxol-5-yl)-2'-oxo-1',2'-dihydrospiro[piperidine-4,3'-pyrrolo[2,3-b]pyridin]-1-yl)hexyl)carbamate (**16**) (75 mg, 0.143 mmol) in DCM (1 mL) at 0 °C, TFA (0.08 mL, 0.718 mmol, 5 equiv.) was added. The resulting reaction mixture was stirred at room temperature for 16 h and monitored by TLC and LC-MS. Upon completion of the reaction, the mixture was concentrated under reduced pressure and co-distilled with diethyl ether. The crude product obtained was 1-(6-aminohexyl)-5'-(benzo[d][1,3]dioxol-5-yl)spiro[piperidine-4,3'-pyrrolo[2,3-b]pyridin]-2'(1'H)-one TFA salt (**17**) (95 mg) as a pale-yellow viscous liquid [51]. This crude product was used in the subsequent step without further purification. LC-MS (ES-API): *m/z* = 422.1 (M+H)⁺.

4.2.4.14. Preparation of 4-((6-(5'-(benzo[d][1,3]dioxol-5-yl)-2'-oxo-1',2'-dihydrospiro[piperidine-4,3'-pyrrolo[2,3-b]pyridin]-1-yl)hexyl)amino)-2-(2,6-dioxopiperidin-3-yl)isoindoline-1,3-dione (Compound 18)

To a stirred solution of 2-(2,6-dioxopiperidin-3-yl)-4-fluoroisoindoline-1,3-dione (**2**) (50 mg, 0.181 mmol) and 1-(6-aminohexyl)-5'-(benzo[d][1,3]dioxol-5-yl)spiro[piperidine-4,3'-pyrrolo[2,3-b]pyridin]-2'(1'H)-one TFA salt (**17**) (76 mg, 0.181 mmol, 1.0 equiv.) in DMSO (1 mL) at RT, was added DIPEA (0.16 mL, 0.90 mmol, 5 equiv.). The reaction mixture was stirred at 100 °C for 1 h and monitored by TLC and LC-MS. After completion, the reaction mixture was cooled, diluted with water (5 mL), and extracted with ethyl acetate (3 × 15 mL). The separated organic layer was washed with water and brine, dried over sodium sulfate, filtered, and concentrated under

reduced pressure to afford the crude product. The crude product was purified by GRACE reverse phase chromatography using 12 g of C18 silica (REVELERIS), eluted with 25-30% acetonitrile/0.1% FA in water. The collected fraction was lyophilized to yield 4-((6-(5'-(benzo[d][1,3]dioxol-5-yl)-2'-oxo-1',2'-dihydrospiro[piperidine-4,3'-pyrrolo[2,3-b]pyridin]-1-yl)hexyl)amino)-2-(2,6-dioxopiperidin-3-yl)isoindoline-1,3-dione (**18**) as a pale-yellow solid (32 mg, 25%). ¹H-NMR (400 MHz, DMSO-d₆): δ 11.08 (bs, 2H), 8.31 (s, 1H), 7.58 (t, *J* = 8.4 Hz, 1H), 7.29 (s, 1H), 7.15-7.07 (m, 2H), 7.01 (t, *J* = 6.8 Hz, 2H), 6.54 (t, *J* = 5.6 Hz, 1H), 6.06 (s, 2H), 5.06-5.02 (m, 1H), 2.92-2.83 (m, 2H), 2.56-2.55 (m, 3H), 2.03-2.00 (m, 3H), 1.95-1.73 (m, 4H), 1.60-1.49 (m, 5H), 1.42-1.32 (m, 5H), 1.23 (s, 9H), 0.85 (t, *J* = 5.6 Hz, 2H); ¹³C-NMR (500 MHz, CD₃OD): 183.1, 175.4, 172.5, 171.7, 170.1, 156.9, 150.8, 149.8, 149.1, 146.6, 138.1, 134.1, 134.0, 132.1, 130.4, 122.4, 118.8, 112.6, 111.9, 110.6, 109.1, 103.5, 59.7, 44.1, 33.0, 32.9, 30.7, 28.7, 28.4, 27.1, 24.6; LC-MS (ES-API): *m/z* = 679.3 (M+H)⁺; IR: 1701.2 cm⁻¹(C=O stretching); MR: 181-185 °C.

4.2.4.15. Preparation of 8-((2-(2,6-dioxopiperidin-3-yl)-1,3-dioxoisindolin-4-yl)amino)octanoic acid (Compound 20)

To a solution of 2-(2,6-dioxopiperidin-3-yl)-4-fluoroisoindoline-1,3-dione (**2**) (150 mg, 0.543 mmol) and 8-aminooctanoic acid (**19**) (95 mg, 0.597 mmol, 1.1 equiv., Alfa Aesar) in DMSO (1.5 mL) at RT, DIPEA (0.28 mL, 1.62 mmol, 3 equiv.) was added. The reaction mixture was stirred at 100 °C for 1 h and monitored by TLC and LC-MS. Upon completion, the reaction mixture was cooled, diluted with 1 N HCl (5 mL), and extracted with ethyl acetate (3 × 10 mL). The separated organic layer was washed with water and brine, dried over sodium sulfate, filtered, and concentrated under reduced pressure to yield the crude product. The crude product was purified by GRACE reverse-phase chromatography using 12 g of C18 silica (REVELERIS), eluted with 50-55% acetonitrile/0.1% FA in water. The collected fraction was concentrated under reduced pressure to afford 8-((2-(2,6-dioxopiperidin-3-yl)-1,3-dioxoisindolin-4-yl)amino)octanoic acid (**20**) (73 mg, 33%) as a green solid. LC-MS (ES-API): *m/z* = 416.2 (M+H)⁺, as reported previously [39].

4.2.4.16. Preparation of 4-((8-(5'-(benzo[d][1,3]dioxol-5-yl)-2'-oxo-1',2'-dihydrospiro[piperidine-4,3'-pyrrolo[2,3-b]pyridin]-1-yl)-8-oxooctyl)amino)-2-(2,6-dioxopiperidin-3-yl)isoindoline-1,3-dione (Compound 21)

To a stirred solution of 5'-(benzo[d][1,3]dioxol-5-yl)spiro[piperidine-4,3'-pyrrolo[2,3-b]pyridin]-2'(1'H)-one (**1**) (55 mg, 0.170 mmol, 1.0 equiv.) in DMF (0.5 mL) at 0 °C under a nitrogen atmosphere, 8-((2-(2,6-dioxopiperidin-3-yl)-1,3-dioxoisindolin-4-yl)amino)octanoic acid (**20**) (70.5 mg, 0.170 mmol, 1.0 equiv.), HATU (97 mg, 0.252 mmol, 1.5 equiv.), and DIPEA (0.08 mL, 0.51 mmol, 3.0 equiv.) were added. The resulting reaction mixture was stirred at room temperature for 2 h and monitored by TLC. After completion, the mixture was diluted with water (3 mL) and extracted with ethyl acetate (3 × 12 mL). The combined organic layers were washed with brine, dried over sodium sulfate, and evaporated to obtain the crude product. The crude product was purified twice by GRACE reverse-phase chromatography using 12 g of C18 silica (REVELERIS), eluted with 35-40% acetonitrile/0.1% ammonium bicarbonate in water. The collected fractions were lyophilized to yield 4-((8-(5'-(benzo[d][1,3]dioxol-5-yl)-2'-oxo-1',2'-dihydrospiro[piperidine-4,3'-pyrrolo[2,3-b]pyridin]-1-yl)-8-oxooctyl)amino)-2-(2,6-dioxopiperidin-3-yl)isoindoline-1,3-dione (**21**) (10 mg, 10%) as a pale-yellow solid. ¹H-NMR (500 MHz, CDCl₃): δ 8.35-8.29 (m, 2H), 8.21 (bs, 1H), 7.62 (d, *J* = 2.5 Hz, 1H), 7.50-7.46 (m, 1H), 7.08 (d, *J* = 7.0 Hz, 1H), 6.97-6.64 (m, 2H), 6.90-6.87 (m, 2H), 6.25-6.24 (m, 1H), 6.02 (s, 2H), 4.91-4.83 (m, 1H), 4.15-4.12 (m, 1H), 4.05-3.95 (m, 1H), 3.95-3.87 (m, 1H), 3.75-3.60 (m, 1H), 3.25 (q, 2H), 2.92-2.87 (m, 1H), 2.81-2.70 (m, 2H), 2.34-2.33 (m, 2H), 2.15-2.10 (m, 1H), 2.05-1.93 (m, 2H), 1.85-1.81 (m, 2H), 1.81-1.71 (m, 4H), 1.44-1.40 (m, 6H); ¹³C-NMR (500 MHz, CD₃OD): 175.5, 175.2, 172.5, 171.7, 150.7, 149.8, 146.3, 138.0, 134.7, 134.1, 134.0, 132.2, 130.8, 122.4, 118.8, 112.5, 110.5, 109.1, 103.5, 44.2, 43.5, 39.3, 34.9, 33.9, 33.0, 31.1, 31.0, 28.6; LC-MS (ES-API): *m/z* = 721.5 (M+H)⁺; IR: 1697.3 cm⁻¹(C=O stretching); MR: 162-164 °C.

4.2.4.17. Preparation of tert-butyl (6-(5'-(benzo[d][1,3]dioxol-5-yl)-2'-oxo-1',2'-dihydrospiro[piperidine-4,3'-pyrrolo[2,3-b]pyridin]-1-yl)hexyl)carbamate (Compound 23)

To a solution of 5'-(benzo[d][1,3]dioxol-5-yl)spiro[piperidine-4,3'-pyrrolo[2,3-b]pyridin]-2'(1'H)-one (**1**) (100 mg, 0.309 mmol) and tert-butyl (2-bromoethyl)carbamate (**22**) (69 mg, 0.309 mmol, 1.0 equiv., Combi) in DMF (1 mL), potassium carbonate (125 mg, 0.928 mmol, 3.0 equiv.) was added. The resulting reaction mixture was stirred at room temperature for 16 h and monitored by TLC and

LC-MS. Upon completion of the reaction, the mixture was diluted with water (5 mL) and extracted with ethyl acetate (2 × 12 mL). The separated organic layer was washed with water and brine, dried over sodium sulfate, filtered, and concentrated under reduced pressure to obtain the crude product. The crude product was purified by GRACE chromatography using 12 g of silica (REVELERIS), eluted with 2-5% methanol in DCM, yielding tert-butyl (6-(5'-(benzo[d][1,3]dioxol-5-yl)-2'-oxo-1',2'-dihydrospiro[piperidine-4,3'-pyrrolo[2,3-b]pyridin]-1-yl)hexyl)carbamate (**23**) as a pale-yellow solid (53 mg, 35%). ¹H-NMR (400 MHz, CDCl₃): δ 8.31 (bs, 1H), 8.28 (s, 1H), 6.99-6.90 (m, 3H) 6.02 (s, 2H), 5.06 (s, 1H), 3.29 (bs, 2H), 2.97 (bs, 2H), 2.64 (m, 4H), 2.10 (bs, 2H), 1.86 (bs, 2H), 1.47 (s, 9H); LC-MS (ES-API): m/z = 467.3 (M+H)⁺.

4.2.4.18. Preparation of 1-(2-aminoethyl)-5'-(benzo[d][1,3]dioxol-5-yl)spiro[piperidine-4,3'-pyrrolo[2,3-b]pyridin]-2'(1'H)-one (Compound 24)

To a solution of tert-butyl (6-(5'-(benzo[d][1,3]dioxol-5-yl)-2'-oxo-1',2'-dihydrospiro[piperidine-4,3'-pyrrolo[2,3-b]pyridin]-1-yl)hexyl)carbamate (**23**) (100 mg, 0.214 mmol) in DCM (1 mL) was added trifluoroacetic acid (0.12 mL, 1.070 mmol, 5 equiv.) at 0 °C. The resulting reaction mixture was stirred at room temperature for 16 h and monitored by TLC and LC-MS. Upon completion of the reaction, the mixture was concentrated under reduced pressure and co-distilled with diethyl ether to yield 1-(2-aminoethyl)-5'-(benzo[d][1,3]dioxol-5-yl)spiro[piperidine-4,3'-pyrrolo[2,3-b]pyridin]-2'(1'H)-one as the TFA salt (**24**) as a pale-yellow viscous liquid (110 mg). This crude product was used in the subsequent step without further purification. LC-MS (ES-API): m/z = 422.1 (M+H)⁺.

4.2.4.19. Preparation of 4-((2-(5'-(benzo[d][1,3]dioxol-5-yl)-2'-oxo-1',2'-dihydrospiro[piperidine-4,3'-pyrrolo[2,3-b]pyridin]-1-yl)ethyl)amino)-2-(2,6-dioxopiperidin-3-yl)isoindoline-1,3-dione (Compound 25)

To a solution of 1-(2-aminoethyl)-5'-(benzo[d][1,3]dioxol-5-yl)spiro[piperidine-4,3'-pyrrolo[2,3-b]pyridin]-2'(1'H)-one TFA salt (**24**) (95 mg, 0.259 mmol, 1.0 equiv.) and 2-(2,6-dioxopiperidin-3-yl)-4-fluoroisoindoline-1,3-dione (**2**) (71 mg, 0.259 mmol, 1.0 equiv.) in DMSO (1.5 mL), DIPEA (0.22 mL, 1.29 mmol, 5.0 equiv.) was added at room temperature. The reaction mixture was stirred at 100 °C for 1 h, with progress monitored by TLC and LC-MS. Upon completion, the mixture was cooled to room

temperature, diluted with water (4 mL), and extracted with ethyl acetate (2 × 10 mL). The organic layer was washed with water and brine, dried over sodium sulfate, filtered, and concentrated under reduced pressure to yield the crude product. The crude product was purified twice by GRACE reverse phase chromatography using 12 g of C18 silica (REVELERIS) and eluted with 32-38% acetonitrile/0.1% formic acid in water. The collected fractions were lyophilized to afford 4-((2-(5'-(benzo[d][1,3]dioxol-5-yl)-2'-oxo-1',2'-dihydrospiro[piperidine-4,3'-pyrrolo[2,3-b]pyridin]-1-yl)ethyl)amino)-2-(2,6-dioxopiperidin-3-yl)isoindoline-1,3-dione (**25**) as a pale yellow solid (70 mg, 21%). ¹H-NMR (500 MHz, CDCl₃): δ 8.49 (bs, 2H), 8.27 (d, *J* = 2.0 Hz, 1H), 7.75 (d, *J* = 1.5 Hz, 1H), 7.51 (t, *J* = 8.0 Hz, 1H), 7.11 (d, *J* = 7.0 Hz, 1H), 6.99-6.98 (m, 2H), 6.93-6.85 (m, 1H), 6.03 (s, 2H), 4.93-4.90 (m, 1H), 3.49-3.43 (m, 2H), 3.10-3.01 (m, 2H), 2.88-2.61 (m, 8H), 2.13-2.04 (m, 5H); ¹³C-NMR (500 MHz, DMSO-*d*₆): 180.6, 172.7, 170.0, 168.8, 167.3, 155.0, 147.9, 146.7, 146.3, 144.1, 136.2, 132.1, 131.8, 129.7, 128.7, 120.1, 117.4, 110.4, 109.2, 108.7, 107.1, 101.1, 55.9, 48.5, 47.9, 45.38, 31.9, 30.9, 22.12; LC-MS (ES-API): *m/z* = 623.3 (M+H)⁺; IR: 1703.1 cm⁻¹ (C=O stretching); MR: 195-199 °C.

4.2.4.20. Preparation of tert-butyl (27-(5'-(benzo[d][1,3]dioxol-5-yl)-2'-oxo-1',2'-dihydrospiro[piperidine-4,3'-pyrrolo[2,3-b]pyridin]-1-yl)-27-oxo-3,6,9,12,15,18,21,24-octaohaheptacosyl)carbamate (Compound 27)

To a stirred solution of 5'-(benzo[d][1,3]dioxol-5-yl)spiro[piperidine-4,3'-pyrrolo[2,3-b]pyridin]-2'(1H)-one (**1**) (60 mg, 0.184 mmol, 1.0 equiv.) in DMF (0.6 mL) at 0 °C under a nitrogen atmosphere, 2,2-dimethyl-4-oxo-3,8,11,14,17,20,23,26,29-nonaoxa-5-azadotriacontan-32-oic acid (**26**) (100 mg, 0.184 mmol, 1.0 equiv.), HATU (104 mg, 0.276 mmol, 1.5 equiv.), and DIPEA (0.09 mL, 0.55 mmol, 3.0 equiv.) were added. The resulting reaction mixture was stirred at room temperature for 2 h, with progress monitored by TLC. After completion, the reaction mixture was diluted with water (4 mL) and extracted with ethyl acetate (3 × 5 mL). The combined organic layers were washed with brine, dried over sodium sulfate, filtered, and concentrated under reduced pressure to yield the crude product. The crude product was purified twice by GRACE reverse phase chromatography using 12 g of C18 silica (REVELERIS) and eluted with 25-30% acetonitrile/0.1% ammonium bicarbonate in water. The collected fractions were lyophilized to afford tert-butyl (27-(5'-(benzo[d][1,3]dioxol-5-yl)-2'-oxo-1',2'-

dihydrospiro[piperidine-4,3'-pyrrolo[2,3-b]pyridin]-1-yl)-27-oxo-3,6,9,12,15,18,21,24-octaoxaheptacosyl)carbamate (**27**) as a pale-yellow solid (55 mg, 32%). ¹H-NMR (400 MHz, CDCl₃): δ 8.28 (d, *J* = 2.0 Hz, 1H), 8.00 (bs, 1H), 7.63 (d, *J* = 2.0 Hz, 1H), 6.96-6.95 (m, 1H), 6.91-6.90 (m, 1H), 6.02 (s, 2H), 5.11 (bs, 1H), 4.20-4.00 (m, 2H), 3.95-3.85 (m, 4H), 3.65-3.61 (m, 30H), 3.55-3.54 (m, 3H), 1.44 (s, 9H); LC-MS (ES-API): *m/z* = 847.5 (M+H)⁺.

4.2.4.21. Preparation of 1-(1-amino-3,6,9,12,15,18,21,24-octaoxaheptacosan-27-oyl)-5'-(benzo[d][1,3]dioxol-5-yl)spiro[piperidine-4,3'-pyrrolo[2,3-b]pyridin]-2'(1'H)-one (Compound 28)

To a stirred solution of tert-butyl (27-(5'-(benzo[d][1,3]dioxol-5-yl)-2'-oxo-1',2'-dihydrospiro[piperidine-4,3'-pyrrolo[2,3-b]pyridin]-1-yl)-27-oxo-3,6,9,12,15,18,21,24-octaoxaheptacosyl)carbamate (**27**) (100 mg, 0.118 mmol, 1 equiv.) in DCM (1 mL), TFA (0.06 mL, 0.591 mmol, 5 equiv.) was added at 0 °C. The reaction mixture was then stirred at room temperature for 16 h, monitored by TLC and LC-MS. After the reaction was complete, the mixture was concentrated under reduced pressure and co-distilled with diethyl ether to obtain 80 mg of 1-(1-amino-3,6,9,12,15,18,21,24-octaoxaheptacosan-27-oyl)-5'-(benzo[d][1,3]dioxol-5-yl)spiro[piperidine-4,3'-pyrrolo[2,3-b]pyridin]-2'(1'H)-one (**28**) TFA salt as a yellow viscous liquid. This material was used in the next step without purification. LC-MS (ES-API): *m/z* = 745.4 (M+H)⁺.

4.2.4.22. Preparation of 4-((27-(5'-(benzo[d][1,3]dioxol-5-yl)-2'-oxo-1',2'-dihydrospiro[piperidine-4,3'-pyrrolo[2,3-b]pyridin]-1-yl)-27-oxo-3,6,9,12,15,18,21,24-octaoxaheptacosyl)amino)-2-(2,6-dioxopiperidin-3-yl)isoindoline-1,3-dione (Compound 29)

To a solution of 2-(2,6-dioxopiperidin-3-yl)-4-fluoroisoindoline-1,3-dione (**2**) (35 mg, 0.128 mmol) and 1-(1-amino-3,6,9,12,15,18,21,24-octaoxaheptacosan-27-oyl)-5'-(benzo[d][1,3]dioxol-5-yl)spiro[piperidine-4,3'-pyrrolo[2,3-b]pyridin]-2'(1'H)-one (**28**) (94 mg, 0.128 mmol) in DMSO (0.5 mL), DIPEA (0.06 mL, 0.384 mmol, 3 equiv.) was added at room temperature. The reaction mixture was then stirred at 100 °C for 1 h, monitored by TLC and LC-MS. After the reaction was complete, the mixture was cooled, diluted with water (2 mL), and extracted with ethyl acetate (3 × 5 mL). The

separated organic layer was washed with water and brine, dried over sodium sulfate, filtered, and concentrated under reduced pressure to afford the crude product. This crude product was purified twice by GRACE reverse phase using 12 g C18 (REVELERIS) eluted with 32-35% acetonitrile/10 mM ammonium bicarbonate in water. The collected fraction was lyophilized to obtain 4-((27-(5'-(benzo[d][1,3]dioxol-5-yl)-2'-oxo-1',2'-dihydrospiro[piperidine-4,3'-pyrrolo[2,3-b]pyridin]-1-yl)-27-oxo-3,6,9,12,15,18,21,24-octaoxaheptacosyl)amino)-2-(2,6-dioxopiperidin-3-yl)isoindoline-1,3-dione (**29**) as a pale yellow solid (21 mg, 19%). **¹H-NMR (500 MHz, DMSO-*d*₆)**: δ 11.11 (s, 1H), 11.10 (s, 1H), 8.33 (d, *J* = 2.0 Hz, 1H), 8.08 (d, *J* = 2.0 Hz, 1H), 7.57 (t, *J* = 7.5 Hz, 1H), 7.31 (d, *J* = 1.5 Hz, 1H), 7.18-7.13 (m, 2H), 7.01 (d, *J* = 7.0 Hz, 1H), 6.98 (d, *J* = 7.0 Hz, 1H), 6.59 (t, *J* = 5.5 Hz, 1H), 6.02 (s, 2H), 5.06-5.02 (m, 1H), 3.87-3.75 (m, 4H), 3.67 (t, *J* = 7.0 Hz, 2H), 3.62 (t, *J* = 5.5 Hz, 2H), 3.56-3.44 (m, 32H), 2.91-2.85 (m, 1H), 2.71-2.65 (m, 1H), 2.62-2.55 (m, 2H), 2.05-1.95 (m, 1H), 1.82-1.74 (m, 4H); **¹³C-NMR (500 MHz, CD₃OD)**: 183.4, 175.5, 173.2, 172.3, 171.5, 156.8, 150.7, 149.8, 149.0, 146.3, 138.1, 134.7, 134.1, 133.9, 132.2, 130.8, 122.4, 119.1, 112.9, 110.6, 109.1, 103.5, 72.4, 72.3, 72.2, 72.1, 71.4, 69.3, 44.1, 43.7, 39.4, 35.3, 34.6, 33.8, 33.0, 24.6; **LC-MS (ES-API)**: *m/z* = 1003.8 (M+H)⁺; **IR**: 1703.1 cm⁻¹(C=O stretching).

4.2.4.23. Preparation of tert-butyl 1-((2-(2,4-dioxotetrahydropyrimidin-1(2H)-yl)-1,3-dioxo-2,3-dihydro-1H-inden-4-yl)amino)-3,6,9,12,15,18-hexaoxahenicosan-21-oate (Compound 31)

To a solution of 2-(2,6-dioxopiperidin-3-yl)-4-fluoroisoindoline-1,3-dione (**2**) (300 mg, 1.08 mmol, 1 equiv.) and tert-butyl 1-amino-3,6,9,12,15,18-hexaoxahenicosan-21-oate (**30**) (467 mg, 1.08 mmol, 1 equiv.) in DMSO (3 mL), DIPEA (1 mL, 3.24 mmol, 3 equiv.) was added. The reaction mixture was then stirred at 100 °C for 1 h, monitored by TLC and LC-MS. After completion of the reaction, the mixture was cooled, diluted with water (10 mL), and extracted with ethyl acetate (3 × 15 mL). The separated organic layer was washed with water and brine, dried over sodium sulfate, filtered, and concentrated under reduced pressure to afford the crude product. This crude product was purified by GRACE reverse phase using 12 g silica (REVELERIS) eluted with 50-55% acetonitrile/0.1% FA in water. The fraction containing the compound was concentrated to afford tert-butyl 1-((2-(2,4-dioxotetrahydropyrimidin-1(2H)-yl)-1,3-

dioxo-2,3-dihydro-1H-inden-4-yl)amino)-3,6,9,12,15,18-hexaoxahenicosan-21-oate (**31**) (205 mg, 28%) as a green solid. ¹H-NMR (400 MHz, CDCl₃): δ 8.19 (s, 1H), 7.81-7.47 (m, 1H), 7.11 (d, J = 7.2 Hz, 1H), 6.92 (d, J = 8.8 Hz, 1H), 6.49-6.48 (m, 1H), 4.93-4.88 (m, 1H), 3.73-3.59 (m, 23H), 3.45 (q, 2H), 2.90-2.65 (m, 2H), 2.14-2.11 (m, 2H), 2.51 (t, 2H), 1.44 (s, 9H); LC-MS (ES-API): m/z = 666.3 (M+H)⁺.

4.2.4.24. Preparation of 1-((2-(2,4-dioxotetrahydropyrimidin-1(2H)-yl)-1,3-dioxo-2,3-dihydro-1H-inden-4-yl)amino)-3,6,9,12,15,18-hexaoxahenicosan-21-oic acid (Compound 32)

To a solution of tert-butyl 1-((2-(2,4-dioxotetrahydropyrimidin-1(2H)-yl)-1,3-dioxo-2,3-dihydro-1H-inden-4-yl)amino)-3,6,9,12,15,18-hexaoxahenicosan-21-oate (**31**) (180 mg, 0.270 mmol, 1 equiv.) in DCM (2 mL), TFA (0.15 mL, 1.35 mmol, 5 equiv.) was added at 0 °C. The resulting reaction mixture was stirred at room temperature for 16 h, and monitored by TLC and LC-MS. After the reaction was complete, the mixture was concentrated under reduced pressure and co-distilled with diethyl ether to obtain 175 mg of 1-((2-(2,4-dioxotetrahydropyrimidin-1(2H)-yl)-1,3-dioxo-2,3-dihydro-1H-inden-4-yl)amino)-3,6,9,12,15,18-hexaoxahenicosan-21-oic acid (**32**) as a yellow viscous liquid. This material was used in the next step without purification. LC-MS (ES-API): m/z = 610.3 (M+H)⁺.

4.2.4.25. Preparation of 1-(4-((21-(5'-(benzo[d][1,3]dioxol-5-yl)-2'-oxo-1',2'-dihydrospiro[piperidine-4,3'-pyrrolo[2,3-b]pyridin]-1-yl)-21-oxo-3,6,9,12,15,18-hexaoxahenicosyl)amino)-1,3-dioxo-2,3-dihydro-1H-inden-2-yl)dihydropyrimidine-2,4(1H,3H)-dione (Compound 33)

To a stirred solution of 5'-(benzo[d][1,3]dioxol-5-yl)spiro[piperidine-4,3'-pyrrolo[2,3-b]pyridin]-2'(1'H)-one (**1**) (80 mg, 0.246 mmol, 1 equiv.) in DMF (2 mL) at 0 °C under a nitrogen atmosphere were added 1-((2-(2,4-dioxotetrahydropyrimidin-1(2H)-yl)-1,3-dioxo-2,3-dihydro-1H-inden-4-yl)amino)-3,6,9,12,15,18-hexaoxahenicosan-21-oic acid (**32**) (150 mg, 0.246 mmol), HATU (140 mg, 0.369 mmol, 1.5 equiv.), and DIPEA (0.13 mL, 0.738 mmol, 3 equiv.). The resulting reaction mixture was stirred at room temperature for 1 h, with the progress of the reaction monitored by TLC. The mixture was then diluted with water (5 mL) and extracted with ethyl acetate (3 × 10 mL). The combined organic layers were washed with brine, dried over sodium sulfate, and

evaporated to obtain the crude product. This product was purified twice by GRACE reverse phase using 12 g C18 (REVELERIS) eluted with 40-45% acetonitrile/10 mM ammonium bicarbonate in water. The collected fraction was lyophilized to obtain 1-(4-((21-(5'-(benzo[d][1,3]dioxol-5-yl)-2'-oxo-1',2'-dihydrospiro[piperidine-4,3'-pyrrolo[2,3-b]pyridin]-1-yl)-21-oxo-3,6,9,12,15,18-hexaoxahenicosyl)amino)-1,3-dioxo-2,3-dihydro-1H-inden-2-yl)dihydropyrimidine-2,4(1H,3H)-dione (**33**) (45 mg, 20%) as an off-white solid. ¹H-NMR (400 MHz, DMSO-d₆): δ 11.11 (bs, 2H), 8.33 (t, J = 2.0 Hz, 1H), 8.08 (d, J = 2.0 Hz, 1H), 7.59-7.55 (m, 1H), 7.31 (d, J = 2.0 Hz, 1H), 7.18-7.12 (m, 2H), 7.03 (d, J = 7.2 Hz, 1H), 6.98 (d, J = 7.2 Hz, 1H), 6.05 (s, 2H), 5.06-5.02 (m, 1H), 3.84-3.77 (m, 4H), 3.65 (t, J = 6.4 Hz, 1H), 3.61 (t, J = 5.2 Hz, 1H), 3.55-3.45 (m, 23H), 2.91-2.81 (m, 1H), 2.67-2.65 (m, 1H), 2.62-2.57 (m, 3H), 2.05-2.00 (m, 1H), 1.85-1.71 (m, 4H); ¹³C-NMR (500 MHz, CD₃OD): 175.2, 173.1, 172.3, 151.5, 149.5, 148.2, 146.3, 138.0, 132.2, 130.9, 122.4, 119.1, 112.8, 110.6, 109.1, 103.5, 72.4, 72.3, 71.4, 69.5, 44.1, 43.7, 35.4, 34.6, 33.8, 33.0, 24.6; LC-MS (ES-API): m/z = 915.3 (M+H)⁺, IR: 1703.1cm⁻¹(C=O stretching); MR: 105-110 °C.

4.3 Computational analysis

4.3.1 Preparation of input files

The PDB files were gathered from the Protein Data Bank (PDB; accessible at <https://www.rcsb.org/>). The CRBN and target protein chains underwent a purification procedure to eliminate any non-protein entities. The 5P9J structure (BTK1 co-crystallized with ibrutinib) was manually extracted from the PDB [29]. When the PROTAC was not present in the structure, other structures with the same domains and ligands were aligned, and the ligand coordinates were duplicated. Hydrogens were added to the ligands using UCSF Chimera, a software tool [40]. After adding the protonated ligands to the structures, side-chain repacking and minimization were performed. To maintain the original coordinates and atom numbering, the ligand was replaced with its minimized equivalent. The SMILES representation of the linker was obtained from the PDB. If the structure was not available in the PDB, it was sourced from the corresponding research article where the structure was first described.

4.3.2 Protein-protein docking

The process of Protein-Protein docking was performed using HADDOCK [41]. The results include solutions to the protein-protein docking problem, which have been organized into clusters based on a 2 Å cut-off. A comprehensive evaluation was conducted on a maximum of 1,000 docking solutions at a global scale for the subsequent phase. Specifically designed for docking, the procedure generates a maximum of 50 local docking outcomes for each global docking solution obtained using HADDOCK.

4.3.3 Generation of constrained PROTAC conformations for docking solutions

RDKit was used to generate up to 100 conformations of the PROTAC, adhering to the constraints imposed by the two ligands to ensure a proper fit within the local docking solution. This sampling process focuses exclusively on the linker conformation, keeping the conformation and position of the two ligands fixed. Due to the atom-distance-based limitations, the generated conformations may not initially align with the positions of ligands, necessitating an additional alignment step. After alignment, a threshold of 0.5 Å RMSD (Root Mean Square Deviation) was used to verify the congruence of each ligand with its corresponding X-ray conformation, ensuring the ligands' conformations accurately match their natural states. The constraints in conformation generation in RDKit are crucial because generated conformations may not fully adhere to the specified constraints, primarily due to the reliance on atom distances during the process. If no suitable conformation is achieved after 1,000 trials, the local docking position is discarded.

4.3.4 Modeling PROTAC within the ternary complex

Rosetta's repack methodology was employed to select the most optimal PROTAC conformation from the set obtained in the preceding stage [29]. In this technique, the side chains of the residues are allowed to undergo rotamer switching. The constrained conformations generated using RDKit are provided as rotamers for the PROTAC, with the first conformation used as the initial rotamer. To align conformations based on a single atom (the nearby atom), the Rosetta Packer algorithm incorporates three virtual atoms with predetermined locations into the set of generated residue conformations. The central virtual atom has coordinates corresponding to the center of mass of the two ligands. Additionally, two other virtual atoms are positioned 1 Å from the central atom

along the x and y axes. The central virtual atom is connected to two additional atoms, referred to as nearby atoms. This connection establishes a consistent 3D alignment, preventing the sampled conformations from being translated and avoiding any lever-arm effects. The repacking process is applied to the PROTAC molecule, and any residual molecules located within 10 Å of it. Following repacking, side-chain minimization was performed on the entire structure, except for the PROTAC molecule. Any models with a final score greater than or equal to 0 were eliminated from further consideration.

4.3.5 Clustering top scoring complexes

The DBSCAN clustering approach was used to group data [42]. Clusters were ranked based on the number of models they contained, assuming that clusters with a higher population correspond to more optimal solutions. The DBSCAN algorithm can operate using either the coordinates of points in n dimensions or a distance matrix with precomputed distances between every pair of points. In this study, C α RMSD values of the moving chain, consistently defined as the target protein, were utilized. Before performing the analysis, pairwise RMSD was calculated between the final solutions to create the distance matrix for the DBSCAN algorithm. The clustering process involved grouping the top 200 solutions, determined based on the interface score provided by Rosetta [43]. This score was calculated by subtracting the energy of the complex from the energy of the individual components after side-chain minimization. These top 200 solutions were selected from a pool of 1,000 final solutions generated using Rosetta's repacking methodology. Clusters were ranked based on the number of structures they contained. For clusters of equal size, the ranking was determined by the average score of the final models. A native cluster was operationally defined as a cluster that includes at least one member with a C α RMSD from the native conformation of less than 4 Å. The cluster reported in the study holds the highest rank among all native clusters.

4.4 Biology

4.4.1 Cell lines

All cell lines were obtained from ATCC (Middlesex, UK) and DSMZ (Braunschweig, Germany). Cells were maintained at 37°C in a humidified incubator (5% CO₂/atmospheric air) in the recommended growth medium, supplemented with 10%

fetal calf serum (Gibco), 1x Penicillin-Streptomycin solution (Diagnovum), 2 mM glutamine (Gibco), 1 mM Sodium bicarbonate (Gibco), 1 mM Sodium pyruvate (Gibco), and 20 mM HEPES (Gibco). All cell lines were routinely authenticated and checked for mycoplasma contamination fortnightly using established protocols in our lab [44].

4.4.2 Cytotoxicity assay

The cytotoxicity of all compounds in cell lines was assessed by a 3-(4,5-dimethylthiazol-2-yl)-5-(3-carboxymethoxyphenyl)-2-(4-sulfophenyl)-2H-tetrazolium reduction assay for 72 h on a robotic high-throughput screening platform (HighResBio, Boston, MA, USA), using a standard protocol established in our lab [45]. IC₅₀ calculation from dose-response curves of compounds was performed using Dotmatics (San Diego, CA, USA), as reported earlier [45].

4.4.3 Drug treatment and cell stimulation

RAMOS and JURKAT cells were plated in 6-well cell culture plates, and treated with compounds at concentrations of 0.5×, 1×, and 2× their IC₅₀ values for 72 h. For bortezomib experiments, RAMOS cells were treated with 2× IC₅₀ concentration of **25** with or without 10 nM bortezomib (Sigma Aldrich) for 24 h. In LPS or IgM stimulation experiments, RAMOS cells were first treated with 2× IC₅₀ concentration of PROTAC **25** for 24 h, followed by stimulation with 1 µg/mL LPS (Sigma Aldrich) or 10 µg/F(ab')₂-Goat anti-Human IgG, IgM (H+L) (Thermo Fisher, Cat #16-5099-85) for 10 min. Drug-untreated cells were treated with DMSO at the same concentration in the highest tested drug concentration (the percentage of DMSO was always less than 0.05%). As detailed below, both untreated and drug-treated cells were then collected and processed for Western blot analysis.

4.4.4 Western blotting

Cells were collected and washed twice with 1× PBS by centrifugation. The pelleted cells were suspended in RIPA buffer (Thermo Fisher Scientific, Massachusetts, USA; Cat #89901) supplemented with protease inhibitors (Cat. #04693116001) and phosphatase inhibitors (Cat. #04906837001) obtained from Roche (Basel, Switzerland). The cells were lysed by sonication (25% amplitude, 5 s off, 10 s on, for 1 min) using a Cup Horn Sonicator (Qsonica, LLC., Connecticut, USA) at 4 °C. The lysed cells were

then centrifuged at 13,000× g for 30 min at 4 °C using a benchtop centrifuge. The supernatant was collected in fresh, pre-chilled Eppendorf tubes and either analyzed immediately or stored at -80 °C for later use. The pelleted cell debris was discarded. The protein concentration in the supernatant was quantified using a BCA Protein Assay (Thermo Fisher Scientific, Massachusetts, USA, Cat. #23223 and Cat. #23224).

Proteins (30-40 µg) were separated by 10% SDS-PAGE and then transferred to a nitrocellulose membrane (Cat # 170-4270; Bio-Rad) using the Trans-Blot Turbo transfer system (Bio-Rad, California, USA). The transferred membranes were blocked in 5% BSA in 1× Tris-Buffered Saline containing 0.1% Tween® 20 detergent for 1 h at room temperature. Blocked membranes were then incubated with primary antibodies for 1 h at room temperature or overnight at 4 °C, followed by incubation with secondary antibodies for 1-2 h at room temperature in the dark. Images of blots were acquired using a Gel Doc XR + Gel Documentation System (Bio-Rad, California, USA) with appropriate filters for Alexa Fluor 488. Unless otherwise specified, all primary antibodies were purchased from Cell Signaling Technology, Inc. (Massachusetts, USA) and included: Total BTK (1:1000; Cat. #3533S), Total ITK (1:1000; Cat. # 2380S), Phospho (Tyr223) BTK (1:1000; Cat # 5082S), M4G3LN Phospho (Tyr551, Tyr511) BTK/ITK (1 µg/mL; Cat. # 14-9015-82; Invitrogen, Massachusetts, USA), Total p38 MAPK (1:1000; Cat # 9212S), Phospho (Thr180/Tyr182) p38 MAPK (1:1000; Cat # 9211S), GAPDH (14 C10) (1:4000; Cat # 2118S), and α -Tubulin (1:2000; Cat # T51687, Sigma Aldrich). All secondary antibodies were purchased from Invitrogen (Massachusetts, USA) and included anti-mouse IgG Alexa Fluor 488 (1:2000; Cat. #A11034) and anti-rabbit IgG Alexa Fluor 488 (1:2000; Cat. #A21202).

4.4.5 Blot analysis and statistical analyses

All blots were analyzed using NIH ImageJ software (Bethesda, Maryland, USA). Total and phosphorylated protein band intensities were normalized to loading control (GAPDH or α -Tubulin), and phosphorylated protein band intensities are expressed as normalized values relative to their respective total protein levels.

All statistical analyses were performed using GraphPad Prism software (version 10; Boston, MA, USA), with differences considered significant at $P < 0.05$. For the

comparison of multiple groups within a single factor, one-way ANOVA was used. Multiple comparisons were performed using Tukey's or Dunnett's tests, as appropriate.

DECLARATION OF COMPETING INTEREST

Naveen Kumar Rampeesa, Rambabu Gundla, Gopal Muddasani, Sreenivasa Anugu, and Viswanath Das are listed as inventors on a published patent application titled 'Azaspirooxindolinone based PROTAC compounds to target ITK and BTK kinases', Indian Patent Application No. 202441059537 A. The remaining authors declare no competing interests.

DATA AVAILABILITY STATEMENT

All data supporting the findings of this study are available in the manuscript or supplementary files.

ACKNOWLEDGEMENTS

Dr. Rambabu Gundla acknowledges DBT-BIRAC (BT/AIR01566/PACE-27/22) for financial assistance and GITAM for the facility. RN and RG thank Aragen Lifesciences Pvt Ltd. Hyderabad, India, for providing computational resources for synthesizing and characterizing all the compounds by NMR, LC-MS, and FT-IR. All biological part of the study was supported in parts by the infrastructural projects (CZ-OPENSOURCE – LM2023052; EATRIS-CZ – LM2023053), the Czech biobank network (BBMRI - LM2023033), the projects National Institute for Cancer Research (Program EXCELES, ID Project No. LX22NPO5102) and National Institute for Neurological Research (Program EXCELES, ID Project No. LX22NPO5107) - Funded by the European Union - Next Generation EU from the Ministry of Education, Youth and Sports of the Czech Republic (MEYS), project TN02000109 (Personalized Medicine: From Translational Research into Biomedical Applications is co-financed with the state support of the Technology Agency of the Czech Republic as part of the National Centers of Competence Program), and project SALVAGE (registration number: CZ.02.01.01/00/22_008/0004644, supported by OP JAK, with co-financing from the EU and the State Budget).

SUPPLEMENTARY DATA

The Supporting Data contains the characterization of all compounds (¹H NMR, ¹³C NMR, HRMS, HPLC, and FT-IR spectra), representative IC₅₀ curves, supplementary cytotoxicity method and table, and images of full western blots.

CREDIT AUTHORSHIP CONTRIBUTION STATEMENT

Naveen Kumar Rampeesa: Methodology, Investigation, Formal analysis, Visualization, Writing – original draft. **Rambabu Gundla:** Writing – review & editing, Supervision, Conceptualization, Funding acquisition. **Gopal Muddasani:** Methodology, Investigation, Formal analysis, Data curation. **Sudhakar T:** Investigation, Formal analysis, Data curation. **Sreenivasareddy Anugu:** Formal analysis, Data curation. **Soňa Gurská:** Methodology, Investigation. **Juan Bautista De Sanctis:** Methodology, Investigation. **Petr Džubák:** Resources, Supervision, Funding acquisition. **Marián Hajdúch:** Resources, Supervision, Funding acquisition. **Viswanath Das:** Methodology, Investigation, Supervision, Conceptualization, Funding acquisition, Writing – review & editing.

REFERENCES

- [1] L.J. Berg, L.D. Finkelstein, J.A. Lucas, P.L. Schwartzberg, Tec Family Kinases in T Lymphocyte Development and Function, *Annu. Rev. Immunol.* 23 (2004) 549–600. <https://doi.org/10.1146/annurev.immunol.22.012703.104743>.
- [2] J.A. Readinger, K.L. Mueller, A.M. Venegas, R. Horai, P.L. Schwartzberg, Tec kinases regulate T-lymphocyte development and function: new insights into the roles of Itk and Rlk/Txk, *Immunol Rev* 228 (2009) 93–114. <https://doi.org/10.1111/j.1600-065X.2008.00757.x>.
- [3] B. Ye, C. Zhou, H. Guo, M. Zheng, Effects of BTK signalling in pathogenic microorganism infections, *Journal of Cellular and Molecular Medicine* 23 (2019) 6522–6529. <https://doi.org/10.1111/jcmm.14548>.
- [4] C. McDonald, C. Xanthopoulos, E. Kostareli, The role of Bruton’s tyrosine kinase in the immune system and disease, *Immunology* 164 (2021) 722–736. <https://doi.org/10.1111/imm.13416>.
- [5] S. Volmering, H. Block, M. Boras, C.A. Lowell, A. Zarbock, The Neutrophil Btk Signalosome Regulates Integrin Activation during Sterile Inflammation, *Immunity* 44 (2016) 73–87. <https://doi.org/10.1016/j.immuni.2015.11.011>.
- [6] L.J. Crofford, L.E. Nyhoff, J.H. Sheehan, P.L. Kendall, The role of Bruton’s tyrosine kinase in autoimmunity and implications for therapy, *Expert Review of Clinical Immunology* 12 (2016) 763–773. <https://doi.org/10.1586/1744666X.2016.1152888>.
- [7] K. Maddocks, Update on mantle cell lymphoma, *Blood* 132 (2018) 1647–1656. <https://doi.org/10.1182/blood-2018-03-791392>.

- [8] E. Dolgin, BTK blockers make headway in multiple sclerosis, *Nature Biotechnology* 39 (2021) 3–5. <https://doi.org/10.1038/s41587-020-00790-7>.
- [9] N. Sahu, A. August, ITK inhibitors in inflammation and immune-mediated disorders, *Curr Top Med Chem* 9 (2009) 690–703. <https://doi.org/10.2174/156802609789044443>.
- [10] A. August, S. Gibson, Y. Kawakami, T. Kawakami, G.B. Mills, B. Dupont, CD28 is associated with and induces the immediate tyrosine phosphorylation and activation of the Tec family kinase ITK/EMT in the human Jurkat leukemic T-cell line., *Proceedings of the National Academy of Sciences* 91 (1994) 9347–9351. <https://doi.org/10.1073/pnas.91.20.9347>.
- [11] A.K. Kannan, D.-G. Kim, A. August, M.S. Bynoe, Itk signals promote neuroinflammation by regulating CD4+ T-cell activation and trafficking, *J Neurosci* 35 (2015) 221–233. <https://doi.org/10.1523/JNEUROSCI.1957-14.2015>.
- [12] K.S. Lechner, M.F. Neurath, B. Weigmann, Role of the IL-2 inducible tyrosine kinase ITK and its inhibitors in disease pathogenesis, *Journal of Molecular Medicine* 98 (2020) 1385–1395. <https://doi.org/10.1007/s00109-020-01958-z>.
- [13] M. Raab, Y.C. Cai, S.C. Bunnell, S.D. Heyeck, L.J. Berg, C.E. Rudd, p56Lck and p59Fyn regulate CD28 binding to phosphatidylinositol 3-kinase, growth factor receptor-bound protein GRB-2, and T cell-specific protein-tyrosine kinase ITK: implications for T-cell costimulation., *Proceedings of the National Academy of Sciences* 92 (1995) 8891–8895. <https://doi.org/10.1073/pnas.92.19.8891>.
- [14] K. Huck, O. Feyen, T. Niehues, F. Rüschenhoff, N. Hübner, H.-J. Laws, T. Teliëps, S. Knapp, H.-H. Wacker, A. Meindl, H. Jumaa, A. Borkhardt, Girls homozygous for an IL-2-inducible T cell kinase mutation that leads to protein deficiency develop fatal EBV-associated lymphoproliferation, *J Clin Invest* 119 (2009) 1350–1358. <https://doi.org/10.1172/JCI37901>.
- [15] J.R. Brown, Ibrutinib (PCI-32765), the First BTK (Bruton's Tyrosine Kinase) Inhibitor in Clinical Trials, *Current Hematologic Malignancy Reports* 8 (2013) 1–6. <https://doi.org/10.1007/s11899-012-0147-9>.
- [16] Y.-T. Tai, B.Y. Chang, S.-Y. Kong, M. Fulciniti, G. Yang, Y. Calle, Y. Hu, J. Lin, J.-J. Zhao, A. Cagnetta, M. Cea, M.A. Sellitto, M.Y. Zhong, Q. Wang, C. Acharya, D.R. Carrasco, J.J. Buggy, L. Elias, S.P. Treon, W. Matsui, P. Richardson, N.C. Munshi, K.C. Anderson, Bruton tyrosine kinase inhibition is a novel therapeutic strategy targeting tumor in the bone marrow microenvironment in multiple myeloma, *Blood* 120 (2012) 1877–1887. <https://doi.org/10.1182/blood-2011-12-396853>.
- [17] A.D. Buhimschi, H.A. Armstrong, M. Toure, S. Jaime-Figueroa, T.L. Chen, A.M. Lehman, J.A. Woyach, A.J. Johnson, J.C. Byrd, C.M. Crews, Targeting the C481S Ibrutinib-Resistance Mutation in Bruton's Tyrosine Kinase Using PROTAC-Mediated Degradation, *Biochemistry* 57 (2018) 3564–3575. <https://doi.org/10.1021/acs.biochem.8b00391>.
- [18] Y. Sun, X. Zhao, N. Ding, H. Gao, Y. Wu, Y. Yang, M. Zhao, J. Hwang, Y. Song, W. Liu, Y. Rao, PROTAC-induced BTK degradation as a novel therapy for mutated BTK C481S induced ibrutinib-resistant B-cell malignancies, *Cell Research* 28 (2018) 779–781. <https://doi.org/10.1038/s41422-018-0055-1>.
- [19] Y.-Q. Li, W.G. Lannigan, S. Davoodi, F. Daryaei, A. Corrionero, P. Alfonso, J.A. Rodriguez-Santamaria, N. Wang, J.D. Haley, P.J. Tonge, Discovery of Novel Bruton's Tyrosine Kinase PROTACs with Enhanced Selectivity and Cellular Efficacy, *J. Med. Chem.* 66 (2023) 7454–7474. <https://doi.org/10.1021/acs.jmedchem.3c00176>.

- [20] D.W. Robbins, A. Kelly, M. Tan, J. McIntosh, J. Wu, Z. Konst, D. Kato, G. Peng, J. Mihalic, D. Weiss, L. Perez, J. Tung, A. Kolobova, S. Borodovsky, R. Rountree, A. Tenn-McClellan, M. Noviski, J. Ye, S. Basham, T. Ingallinera, J. McKinnell, D.E. Karr, J. Powers, C. Guiducci, A. Sands, Nx-2127, a Degradable of BTK and IMiD Neosubstrates, for the Treatment of B-Cell Malignancies, *Blood* 136 (2020) 34–34. <https://doi.org/10.1182/blood-2020-141461>.
- [21] K.R. Senwar, P. Sharma, T.S. Reddy, M.K. Jeengar, V.L. Nayak, V.G.M. Naidu, A. Kamal, N. Shankaraiah, Spirooxindole-derived morpholine-fused-1,2,3-triazoles: Design, synthesis, cytotoxicity and apoptosis inducing studies, *European Journal of Medicinal Chemistry* 102 (2015) 413–424. <https://doi.org/10.1016/j.ejmech.2015.08.017>.
- [22] P.B. Sampson, Y. Liu, B. Forrest, G. Cumming, S.-W. Li, N.K. Patel, L. Edwards, R. Laufer, M. Feher, F. Ban, D.E. Awrey, G. Mao, O. Plotnikova, R. Hodgson, I. Beletskaya, J.M. Mason, X. Luo, V. Nadeem, X. Wei, R. Kiarash, B. Madeira, P. Huang, T.W. Mak, G. Pan, H.W. Pauls, The Discovery of Polo-Like Kinase 4 Inhibitors: Identification of (1R,2S)-2-(3-((E)-4-(((cis)-2,6-Dimethylmorpholino)methyl)styryl)-1H-indazol-6-yl)-5'-methoxy Spiro[cyclopropane-1,3'-indolin]-2'-one (CFI-400945) as a Potent, Orally Active Antitumor Agent, *J. Med. Chem.* 58 (2015) 147–169. <https://doi.org/10.1021/jm5005336>.
- [23] Y. Zhao, S. Yu, W. Sun, L. Liu, J. Lu, D. McEachern, S. Shargary, D. Bernard, X. Li, T. Zhao, P. Zou, D. Sun, S. Wang, A Potent Small-Molecule Inhibitor of the MDM2–p53 Interaction (MI-888) Achieved Complete and Durable Tumor Regression in Mice, *J. Med. Chem.* 56 (2013) 5553–5561. <https://doi.org/10.1021/jm4005708>.
- [24] M.S. Altowyan, S.M. Soliman, M. Haukka, N.H. Al-Shaalan, A.A. Alkharboush, A. Barakat, Synthesis, Characterization, and Cytotoxicity of New Spirooxindoles Engrafted Furan Structural Motif as a Potential Anticancer Agent, *ACS Omega* 7 (2022) 35743–35754. <https://doi.org/10.1021/acsomega.2c03790>.
- [25] S. Vollmer, D. Cunoosamy, H. Lv, H. Feng, X. Li, Z. Nan, W. Yang, M.W.D. Perry, Design, Synthesis, and Biological Evaluation of MEK PROTACs, *J. Med. Chem.* 63 (2020) 157–162. <https://doi.org/10.1021/acs.jmedchem.9b00810>.
- [26] G. Mudasani, K. Paidikondala, S. Gurská, S.J. Maddirala, P. Džubák, V. Das, R. Gundla, C-5 Aryl Substituted Azaspirooxindolinones Derivatives: Synthesis and Biological Evaluation as Potential Inhibitors of Tec Family Kinases, *European Journal of Organic Chemistry* 2021 (2021) 4630–4640. <https://doi.org/10.1002/ejoc.202100699>.
- [27] S. Kregel, C. Wang, X. Han, L. Xiao, E. Fernandez-Salas, P. Bawa, B.L. McCollum, K. Wilder-Romans, I.J. Apel, X. Cao, C. Speers, S. Wang, A.M. Chinnaiyan, Androgen receptor degraders overcome common resistance mechanisms developed during prostate cancer treatment, *Neoplasia* 22 (2020) 111–119. <https://doi.org/10.1016/j.neo.2019.12.003>.
- [28] Z. Liu, M. Hu, Y. Yang, C. Du, H. Zhou, C. Liu, Y. Chen, L. Fan, H. Ma, Y. Gong, Y. Xie, An overview of PROTACs: a promising drug discovery paradigm, *Molecular Biomedicine* 3 (2022) 46. <https://doi.org/10.1186/s43556-022-00112-0>.
- [29] A.T. Bender, A. Gardberg, A. Pereira, T. Johnson, Y. Wu, R. Grenningloh, J. Head, F. Morandi, P. Haselmayer, L. Liu-Bujalski, Ability of Bruton's Tyrosine Kinase Inhibitors to Sequester Y551 and Prevent Phosphorylation Determines Potency

- for Inhibition of Fc Receptor but not B-Cell Receptor Signaling, *Mol Pharmacol* 91 (2017) 208. <https://doi.org/10.1124/mol.116.107037>.
- [30] C.P. Koraboina, V.C. Maddipati, N. Annadurai, S. Gurská, P. Džubák, M. Hajdúch, V. Das, R. Gundla, Synthesis and Biological Evaluation of Oxindole Sulfonamide Derivatives as Bruton's Tyrosine Kinase Inhibitors**, *ChemMedChem* n/a (2023) e202300511. <https://doi.org/10.1002/cmdc.202300511>.
- [31] R.D. Medh, M.S. Webb, A.L. Miller, B.H. Johnson, Y. Fofanov, T. Li, T.G. Wood, B.A. Luxon, E.B. Thompson, Gene expression profile of human lymphoid CEM cells sensitive and resistant to glucocorticoid-evoked apoptosis, *Genomics* 81 (2003) 543–555. [https://doi.org/10.1016/S0888-7543\(03\)00045-4](https://doi.org/10.1016/S0888-7543(03)00045-4).
- [32] L. Ping, N. Ding, Y. Shi, L. Feng, J. Li, Y. Liu, Y. Lin, C. Shi, X. Wang, Z. Pan, Y. Song, J. Zhu, The Bruton's tyrosine kinase inhibitor ibrutinib exerts immunomodulatory effects through regulation of tumor-infiltrating macrophages, *Oncotarget*; Vol 8, No 24 (2017). <https://www.oncotarget.com/article/16836/text/> (accessed January 1, 2017).
- [33] S. Nisitani, R.M. Kato, D.J. Rawlings, O.N. Witte, M.I. Wahl, In situ detection of activated Bruton's tyrosine kinase in the Ig signaling complex by phosphopeptide-specific monoclonal antibodies, *Proceedings of the National Academy of Sciences* 96 (1999) 2221–2226. <https://doi.org/10.1073/pnas.96.5.2221>.
- [34] D. Akasaka, S. Iguchi, R. Kaneko, Y. Yoshiga, D. Kajiwara, Y. Nakachi, N. Noma, K. Tanaka, A. Shimizu, F. Hosoi, Novel Bruton's tyrosine kinase inhibitor TAS5315 suppresses the progression of inflammation and joint destruction in rodent collagen-induced arthritis, *PLOS ONE* 18 (2023) e0282117. <https://doi.org/10.1371/journal.pone.0282117>.
- [35] G. Mudasani, K. Paidikondala, R. Gundla, S. Joseph Maddirala, V. Das, Synthesis and Biological Evaluation of 5'-Arylspiro[piperidine-4,3'-pyrrolo-[2,3-b]pyridin] Analogues, *ChemistrySelect* 6 (2021) 3378–3381. <https://doi.org/10.1002/slct.202004719>.
- [36] J. Qi, S. Armstrong, L. Wu, Compounds, compositions, and methods for protein degradation, WO2020264172A1, 2020. <https://patents.google.com/patent/WO2020264172A1/en?q=+WO2020%2f264172> (accessed June 7, 2024).
- [37] H. Wang, C. HUO, Y. GUO, R. QI, Z. Wang, Degradation of bruton's tyrosine kinase (btk) by conjugation of btk inidbitors with e3 ligase ligand and methods of use, WO2021018018A1, 2021. <https://patents.google.com/patent/WO2021018018A1/en?q=WO2021018018> (accessed June 7, 2024).
- [38] X. Zhang, D. Thummuri, X. Liu, W. Hu, P. Zhang, S. Khan, Y. Yuan, D. Zhou, G. Zheng, Discovery of PROTAC BCL-XL degraders as potent anticancer agents with low on-target platelet toxicity, *European Journal of Medicinal Chemistry* 192 (2020) 112186. <https://doi.org/10.1016/j.ejmech.2020.112186>.
- [39] Lun R., Fengying Z., Xiuyun S., Gang Z., Zimo Y., Yonghui S., Xuemei L., Preparation of isoindoline derivatives as degradation agent targeting both BTK and GSPT1 proteins and its application, CN115304606A, 2022. <https://patents.google.com/patent/CN115304606A/zh?q=CN115304606> (accessed June 7, 2024).
- [40] E.F. Pettersen, T.D. Goddard, C.C. Huang, G.S. Couch, D.M. Greenblatt, E.C. Meng, T.E. Ferrin, UCSF Chimera—A visualization system for exploratory

- research and analysis, *Journal of Computational Chemistry* 25 (2004) 1605–1612. <https://doi.org/10.1002/jcc.20084>.
- [41] G.C.P. van Zundert, J.P.G.L.M. Rodrigues, M. Trellet, C. Schmitz, P.L. Kastiris, E. Karaca, A.S.J. Melquiønd, M. van Dijk, S.J. de Vries, A.M.J.J. Bonvin, The HADDOCK2.2 Web Server: User-Friendly Integrative Modeling of Biomolecular Complexes, *Journal of Molecular Biology* 428 (2016) 720–725. <https://doi.org/10.1016/j.jmb.2015.09.014>.
- [42] M. Ester, H.-P. Kriegel, J. Sander, X. Xu, A density-based algorithm for discovering clusters in large spatial databases with noise, in: 1996: pp. 226–231.
- [43] S.J. Fleishman, A. Leaver-Fay, J.E. Corn, E.-M. Strauch, S.D. Khare, N. Koga, J. Ashworth, P. Murphy, F. Richter, G. Lemmon, J. Meiler, D. Baker, RosettaScripts: A Scripting Language Interface to the Rosetta Macromolecular Modeling Suite, *PLOS ONE* 6 (2011) e20161. <https://doi.org/10.1371/journal.pone.0020161>.
- [44] R. Buriánová, J. Kotulová, Detection of mycoplasma contamination in cell lines by PCR, in: J. Drábek, V. Das, P. Dzubak, Josef Strovnal, J. Bouchal, M. Hajduch, K. Koberna, A. Ligasová, M. Mistrik, J. De Sanctis (Eds.), *Laboratory Techniques in Cellular and Molecular Medicine* (1st ed.), Palacký University Olomouc, Olomouc, 2021, pp. 37 – 42. <https://doi.org/10.5507/lf.22.24460499>.
- [45] S. Gurská, Analysis of cytotoxicity by tetrazolium salt reduction test, in: J. Drábek, V. Das, P. Dzubak, Josef Strovnal, J. Bouchal, M. Hajduch, K. Koberna, A. Ligasová, M. Mistrik, J. De Sanctis (Eds.), *Laboratory Techniques in Cellular and Molecular Medicine* (1st ed.), Palacký University Olomouc, Olomouc, 2021, pp. 67 – 72. <https://doi.org/10.5507/lf.22.24460499>.